



Preparation of biodegradable iron scaffolds with controlled porosity for application in orthopaedic devices

Beatriz Duarte de Oliveira Gonçalves

Thesis to obtain the Master of Science Degree in

Materials Engineering

Supervisors: Prof. Maria Amélia Martins de Almeida and Prof. Jie Zhou

Examination Committee

Chairperson: Prof. Luís Filipe da Silva dos Santos

Supervisor: Prof. Maria Amélia Martins de Almeida

Member of the Committee: Prof. Rui Mário Correia da Silva Vilar

December 2014

Abstract

Biodegradable materials for medical applications, that will naturally exit the physiological system after fulfilling their job, sound appealing so as to avoid problems caused by the long-time stay of an implant in the human body. For this purpose iron has been investigated since it is an essential element for the function of the human body. The most studied applications are in the cardiovascular field, and in this case, iron-based materials present the problem of having a degradation rate that is slower than the desired one. On the other hand, the degradation rate of iron may be suitable for the orthopaedic field, where a slower degradation rate is desired. There are very few studies on this matter, which suggests that this is an interesting area for investigation. The goal of this thesis is to study the suitability of using biodegradable iron for orthopaedic implant applications. An iron-based material has been developed by hot pressing and then characterized in terms of porosity, microstructure, mechanical behaviour and corrosion behaviour. The hot pressing technique has been proven to be suitable for processing iron and the corrosion rates achieved in this work seem suitable for the application referred. However, for those levels of biodegradability to be achieved a great compromise in mechanical properties had to be made, which, ultimately, made this material unsuitable for orthopaedic devices therefore, further research is recommended to be toward improving the mechanical properties of iron-based materials while controlling porosity and degradation rate.

Keywords: Iron, porosity, hot pressing, biodegradable orthopaedic implants

Resumo

Materiais biodegradáveis para aplicações médicas que irão, naturalmente, sair do corpo após ter cumprido a sua função é atraente, especialmente para evitar problemas causados pela longa permanência desse implante no corpo humano. O ferro tem sido investigado como material para estas aplicações, já que é um elemento essencial para o bom funcionamento do corpo humano. A área de estudos que mais extensivamente abordou este assunto é a cardiovascular, onde os materiais ferrosos desenvolvidos apresentam uma taxa de corrosão demasiado lenta para este tipo de implantes. Por outro lado, para implantes ortopédicos, a taxa de corrosão necessária é menor, e o ferro pode ser apropriado para este propósito. Atualmente, não existem muitos estudos efetuados sobre este tipo de aplicação, o que sugere que esta área pode ser interessante para aprofundar conhecimentos. O objetivo desta dissertação é estudar a adequabilidade de utilizar ferro como material para implantes ortopédicos biodegradáveis. Desenvolveram-se amostras de um material ferroso por prensagem a quente, seguindo-se a respetiva caracterização em termos de porosidade, microestrutura, propriedades mecânicas e comportamento à corrosão. A técnica utilizada para a fabricação das amostras mostrou-se adequada ao material utilizado e, as taxas de corrosão obtidas mostram melhorias em comparação com estudos anteriores. No entanto, ao melhorar o comportamento à corrosão através da incorporação de porosidade nas amostras, as propriedades mecânicas foram fortemente afetadas, tornando este material inadequado para aplicações ortopédicas. Assim, são recomendadas investigações futuras no sentido de melhorar as propriedades mecânicas deste tipo de materiais, mantendo a porosidade e taxa de corrosão controladas.

Palavras-chave: Ferro, porosidade, prensagem a quente, implante ortopédico biodegradável

Acknowledgements

I would like to thank my supervisors, Professor Maria Amélia Almeida and Professor Jie Zhou, for their guidance and assistance throughout this entire project.

In addition, I would also like to thank Sander Leeflang and Sina Dezfuli, whose help in terms of technical knowledge was essential for the development of this work.

I thank Instituto Superior Técnico and Delft University of Technology for the opportunity of working in two very stimulating academic environments.

I would like to thank Simon, Tugcenur and Mina for all the support, patience and friendship that made my life in Delft an unforgettable experience.

A special thanks to all my friends in Lisbon, for this fantastic journey that is university and for all the support that you gave me in the past years.

Finally, I would like to thank my family for being here for me all these years and for supporting my choices throughout my academic path.

Index

Abstract.....	iii
Resumo	v
Acknowledgements	vii
Index	ix
List of figures	xi
List of tables	xi
1. Introduction	1
2. Biodegradable implants	2
2.1 Properties of biodegradable implants	2
2.1.1 Biocompatibility.....	2
2.1.2 Mechanical properties	3
2.1.3 Degradation properties	3
2.1.4 Surface properties	4
2.2 Materials for biodegradable implants	5
3. Properties of Fe-based biodegradable materials	7
3.1 Degradation Process	7
3.2 Toxicity of degradation products.....	8
3.3 Interaction with cells	9
3.3.1 <i>In vitro</i> studies.....	9
3.3.2 <i>In vivo</i> studies	9
3.4 Mechanical properties	10
3.5 Production methods.....	12
3.5.1 Powder metallurgy.....	12
3.5.2 Hot pressing technique	13
4. Materials and Methods	15
4.1 Sample preparation	15
4.2 Porosity measurements.....	16
4.3 Static corrosion tests	17
4.4 Electrochemical corrosion tests.....	17
4.5 Diametrical compression tests.....	18

4.6	Microstructural characterization.....	18
5.	Results.....	19
5.1	As-pressed samples characterization	19
5.1.1	Microstructure	19
5.1.2	Porosity.....	21
5.1.3	Electrochemical behaviour	22
5.1.4	Mechanical behaviour.....	24
5.2	Characterization of samples after immersion tests	25
5.2.1	Microstructure	25
5.2.2	Mechanical behaviour.....	31
6.	Discussion	32
7.	Conclusions and future work	36
8.	References	37

List of figures

Figure 1: Schematic diagram illustrating the degradation behaviour and evolution of mechanical integrity in biodegradable metal stents [5].....	3
Figure 2: Schematic diagram illustrating the degradation behaviour and evolution of mechanical integrity in biodegradable metal implants in bone [5]	4
Figure 3: General steps of a PM process [38].....	13
Figure 4: General steps of Hot Pressing technique: 1) Insert the powder in the die; 2) Apply a pre-pressure; 3) Heat the die, until the temperature stabilizes; 4) Apply pressure; 5) After cooling the sample is retrieved; 6) Final sample.	14
Figure 5: SEM image of iron powder	15
Figure 6: Schematic of sample shape and sizes after hot pressing	16
Figure 7: Schematic illustration of the configuration of sample and holders for the diametrical compression tests.....	18
Figure 8: SEM micrographs of samples pressed at a) 100 °C, b) 200 °C and c) 400 °C	19
Figure 9: EDS results of the as-pressed samples	20
Figure 10: Bulk porosity of samples produced by hot pressing at different temperatures.	21
Figure 11: Surface porosity of samples produced by hot pressing at different temperatures.	21
Figure 12: Open potential curves of samples pressed at 200 °C.....	22
Figure 13: Open potential curves of samples pressed at 400 °C.....	22
Figure 14: Potentiodynamic curves of samples pressed at 200 °C	23
Figure 15: Potentiodynamic curves of samples pressed at 400 °C	23
Figure 16: As-pressed samples' compression results	24
Figure 17: SEM images of iron processed at 100 °C: a) as-pressed; b) after immersion for 7 days; c) after immersion for 30 days.	26
Figure 18: EDS analysis results of a sample pressed at 100 °C after different immersion periods.....	26
Figure 19: SEM images of iron processed at 200 °C: a) as-pressed; b) after immersion for 7 days; c) after immersion for 15 days; d) after immersion for 30 days.	27
Figure 20: EDS analysis results of a sample pressed at 200 °C after different immersion periods.....	28
Figure 21: SEM images of iron processed at 400 °C: a) as-pressed; b) after immersion for 7 days; c) after immersion for 15 days; d) after immersion for 30 days.	29
Figure 22: EDS analysis results of a sample pressed at 400 °C after different immersion periods.....	30
Figure 23: Results of diametrical compression tests	31
Figure 24: Schematic of corrosion mechanism of iron in salt water at 50 °C after: a) 10 minutes; b) 180 minutes; c) 360 minutes; d) 27 hours [59].....	34

List of tables

Table 1: Corrosion rate values for Fe-based materials tested under Hanks solution environment. a) Electroformed iron; b) Equal Channel Angular Pressing iron	8
Table 2: Mechanical properties of various materials. a) Electroformed Fe; b) Equal Channel Angular Pressure Fe	11

Table 3: Composition of Hank's Balanced Salt Solution	17
Table 4: Results of the Tafel extrapolation method.....	24

1. Introduction

Materials in the medical field have been of great importance and, with the evolution of technology, the search for better performing and safer materials have been increasing over time. Biomaterials and their applications go back as far as thousands of years in the history of mankind [1]. The use of metallic biomaterials had a big impulsion in the 1920s, with the invention of stainless steel [2]. Since then, several metallic materials have been developed and applied to the medical field.

The idea of biodegradable implants came with the awareness that many of the implants used in medicine are only needed to remain in the human body for a short period of time. The solution for that would be for the biomaterial to naturally degrade after fulfilling its objective [3]. Several materials have been studied for this purpose, such as polymeric and metal based materials; nevertheless the metallic materials like iron and magnesium show the most promising outcomes [4-6].

Despite being the most popular materials for biodegradable implants, Fe and Mg still face some problems critical for the application: iron has a very slow degradation rate and magnesium degrades too fast. To overcome these problems research has been carried out involving alloying and structure modification but there is still a lot to be done to reach material properties adequate for the application [4].

Iron has not been studied as much as magnesium although it presents some important characteristics that are absent in magnesium and that are important, especially for orthopaedic applications, such as mechanical and degradation properties [5].

The question that arises is can an iron implant have the appropriate mechanical properties for a period of time sufficient to fulfil its purpose and then degrade in a non-toxic manner?

The aim of this study is to investigate the possibility of developing porous Fe-based materials with increased degradation rate potentially able to be used as biodegradable scaffolds for orthopaedic applications. This study involves the preparation of Fe-based materials by hot pressing technique and the respective characterization in terms of porosity, microstructure, mechanical behaviour and biodegradation behaviour.

The work developed in this thesis has been carried out at Delft University of Technology in Delft, the Netherlands, under the Erasmus program.

2. Biodegradable implants

Biodegradable implants appear as an opposite to corrosion resistant implants. For many years materials for implants aimed at resisting corrosion as long as possible in the body, however, it was realised that for some applications their presence was only needed for a limited period of time. In fact, corrosion-resistant materials that are used for temporary purposes often need to be removed, which implies a second surgical procedure. Furthermore, some of the implants that are allowed to remain in the body can cause health problems in the long term [7].

Biodegradable implants appear as a solution to these health problems, and they are, as the name says, implants made of biodegradable materials, which means that after a period of time, wherein the healing process occurs, they will naturally corrode and exit the physiological system through biological fluids such as urine. This property is not trivial and for a material to be eligible it has to fulfil some specific criteria that vary according to the application.

The use of biodegradable materials is relevant in several medical applications such as orthopaedics and cardiovascular implants, and also includes paediatric applications. This is because most of the implants used in these fields are only needed for a short period of time, after which they are no longer needed.

In the orthopaedic field, for example, bone fixation pins or screws are often required to join the damaged bone and are only necessary until bone tissue has grown enough to sustain the bone structure. For cardiovascular implants the mechanical properties are important in the first stage after implantation, so the corrosion rate must be such that it does not affect these properties. On the other hand, if one considers paediatric applications, the growing tissue environment also needs to be taken into account. Despite the fact that, for different applications, the requirements are different, a common factor in all of them is biodegradability, biocompatibility and non-toxicity of the corrosion products [2].

2.1 Properties of biodegradable implants

Despite the specific requirements for different applications, some properties are common to all biodegradable implants, and the most important ones are presented here.

2.1.1 Biocompatibility

Biocompatibility is a common requirement for all materials in medical applications; it means that a material needs to be able to do its job without causing any harm to the surrounding tissue and the host. By no harm one means that it has to be non-toxic, non-allergic, non-carcinogenic or non-pyrogenic, it cannot cause an inflammatory response and it needs to have good blood compatibility.

Since all the applications involve the contact with biological environment biocompatibility is the first requirement to be considered. The choice of a biocompatible material is of extreme importance in order to assure successful implantation [8].

2.1.2 Mechanical properties

Mechanical support to the surrounding tissue is required in all applications of these materials. Since the implant is going to degrade itself, it is expected that its mechanical integrity becomes compromised over time, but it's important to assure that mechanical properties are not compromised before the healing process is completed. Additionally, some medical procedures require some flexibility of the implant during surgery which cannot compromise its performance.

Taken the examples referred earlier, orthopaedic implants should be able to withstand more mechanical load than a coronary stent for cardiovascular application, since the mechanical load for cortical bone is between 0 to 40 MPa and the arterial wall is only 0.2 to 1 MPa [2]. This implies that according to the tissue that is being replaced, the mechanical requirements will vary.

Regardless of that, mechanical failure is one problem to avoid, and this can be done by creating implants that have characteristics similar to the surrounding tissue, such as strength, stiffness, density and fatigue properties.

2.1.3 Degradation properties

Degradation may be unwanted in most cases but here it is desired. The corrosion rate is an important parameter that needs to be strictly controlled, not only to ensure that the implant fulfils its objective before it starts to degrade but also to guarantee that the material does not stay too long in the body. This means that there will have to be an optimum degradation rate for the material as it cannot be too fast or too slow.

If one takes, for example, the cardiovascular field, more specifically implants such as coronary stents, it was proven that they are only needed for a period of 6 to 12 months [9], after that, healing has already taken place and the stent is no longer needed. As shown in *Figure 1*, the time for the stent to fully degrade is considered to be 12 to 24 months [10].

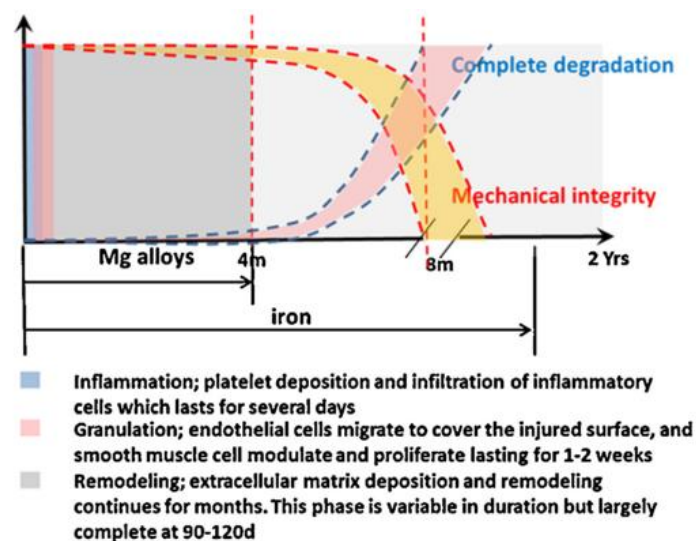


Figure 1: Schematic diagram illustrating the degradation behaviour and evolution of mechanical integrity in biodegradable metal stents [5]

Furthermore, it is possible to observe in this figure that in the first months the implant should either degrade at a very slow rate or not degrade at all, and after the remodelling process, it is ideal for the implant to degrade faster, under the condition that the corrosion products must be under the limits of toxicity.

Two materials are referred here, magnesium alloys and iron, with respect to their degradation rates as coronary stents. It is clear that Mg alloys have a faster corrosion rate than Fe.

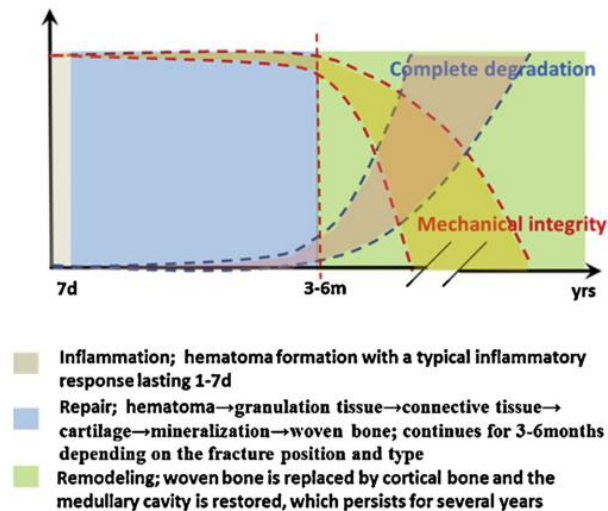


Figure 2: Schematic diagram illustrating the degradation behaviour and evolution of mechanical integrity in biodegradable metal implants in bone [5]

On the other hand, for bone implants, mechanical integrity should become compromised between 6 and 18 months after implantation [11], which means that mechanical integrity needs to be kept for a longer time than in the previous example, and, as a consequence, the degradation rate should be slower so the implant lasts at least until the remodelling process occurs (*Figure 2*).

Furthermore, the way the material corrodes also needs to be taken into account. It's preferable to have uniform corrosion in the implant than localised corrosion because localised corrosion could compromise the effectiveness of the implant, since it could compromise the mechanical integrity of the implant [5].

Summarising, degradability must be such that mechanical integrity is ensured for a period of time between 6 to 18 months for orthopaedic applications, and this will depend not only on the material used, but also on the surface that it presents.

2.1.4 Surface properties

Surface properties will determine how the corrosion process starts, but most importantly, they will determine cell interactions with the implant, such as promptness to cell attachment. The ability to cause cell attachment depends on material surface properties, such as texture. Some studies have been conducted on this topic and the results show that the appropriate surface for specific implant sites, for instance, if the implant is to be in contact with blood stream, is a smooth surface to discourage protein adsorption. However, for bone tissue applications, rough surfaces are reported to promote higher cell anchorage than smooth ones [12].

Besides physical parameters such as surface roughness, chemical composition will also influence cell adsorption at the surface. Surfaces are composed of molecules or atoms and when they have not fully strained bonds, there is an increased reactivity with the biological environment, thus contributing to higher surface energy. Certain chemical groups may induce stronger attraction for certain proteins, which happens with polar/apolar groups. This is related to the hydrophilicity (or hydrophobicity) of the materials surfaces and surface energy is responsible for these phenomena.

Surface energy relates to the wettability of the material. It is desirable to have a lower surface energy, since the higher it is, the more likely it is for adverse events to occur, such as thrombosis¹ [8].

Furthermore rougher surfaces also lead to thrombosis, which implies that not only polishing techniques should be applied but also special care should be taken when using coatings, since coating techniques may affect the surface texture [12].

In what concerns surface potential, there has been some controversy in literature. Despite the fact that most metals are electropositive and biological elements have the tendency to be electronegative, the expected result of increased thrombogenicity towards these materials is not always observed. This means that this factor may influence cell attachment but what will ultimately count is the combination of all the surface properties of the material.

In order to optimise the surface properties, one can modify the surface of the implant itself or apply a coating on it. Coatings can considerably improve surface properties and, as long as the bulk material is not compromised, they can be a viable option [8, 13].

2.2 Materials for biodegradable implants

Most biomaterials are designed for corrosion resistance and the idea of using biodegradable materials for some applications is still quite recent. The most studied biodegradable metals are magnesium and iron-based materials. They were chosen due to their biological functions in the human body, since both metals are necessary for the functioning of the body [5, 14].

In choosing the appropriate material for a biodegradable implant, not only the previously mentioned properties must be taken into consideration, but also the respective processability. This means that the material should have the ability to be formed into an implant with an appropriate shape.

Most of the studies on these materials are focused in one specific application: coronary stents for cardiovascular implantation [7, 10, 13, 15-18]. This is due to the extensive studies that researchers have carried out over the past years in this field. Consequently, more information is available concerning biodegradable materials for this specific application than for others.

Magnesium has been proven to be suitable for coronary stents however, it still shows some problems regarding the too high degradation rate [5]. As far as Fe-based materials are concerned, in vivo tests conducted until now show a degradation rate that is too slow for cardiovascular applications

¹ Thrombosis is the obstruction of the flow in the blood system by means of the formation of a blood clot.

[19]. Despite that, positive results have been achieved, and the non-toxicity and compatibility of iron with living tissue have been proven [20].

These promising results gave rise to the recent growing interest in considering iron-based materials for orthopaedic applications as well. In this field, iron alloys have not been given much attention and there are few studies on the topic. However, the potential is strong since the degradation rate of iron is lower than that required for coronary stents, but appropriate to orthopaedic applications where a slower corrosion rate is necessary. Furthermore, Fe alloys show better mechanical properties than Mg alloys, which are required for load-bearing applications in orthopaedic implants. Mg doesn't seem to be appropriate for orthopaedic applications due not only to the insufficient mechanical properties, but also its fast degradation rate.

3. Properties of Fe-based biodegradable materials

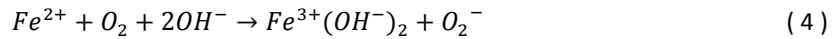
3.1 Degradation Process

It was previously mentioned that uniform corrosion throughout the surface of the implant is preferable over localised corrosion. Studies performed have demonstrated that iron shows uniform corrosion and the chemical reactions that occur on the surface of a Fe-based implant have been deduced as well.

According to the authors [21-23], the degradation process of iron starts when oxidation starts. It consists of an electrochemical process that starts with the following anodic and cathodic reactions:



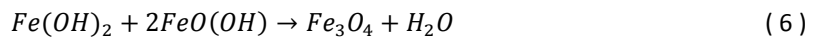
The formation of Fe^{2+} can give rise to two other reactions: either it forms ferrous hydroxide (*reaction 3*), or it can be transformed into Fe^{3+} (*reaction 4*), if oxygen and an alkaline pH are present.



Fe^{3+} can then react to form ferritic hydroxide:



In the presence of oxygen and chloride ions, $FeO(OH)$ precipitates and the formation of magnetite (Fe_3O_4) occurs:



In *in vitro* tests [22, 24], a layer of precipitated degradation products forms, which usually exhibits a brownish colour and consists of the hydroxides originated from the reactions above.

Besides the process itself, the degradation rate of the material is of great importance. The degradation has to be slow enough so that the implant could guarantee mechanical integrity over the time of the healing process, and fast enough so that it would not cause any damage related to extended stay in the body. Taken that into account it is necessary to determine the degradation rate, the mechanical properties, the toxicity related to extended stay of the implant and, the toxicity caused by the corrosion products.

In vitro studies show that the corrosion rate of iron varies from 0,02 to 0,85 mm/year (*Table 1*). These values vary according to the production steps that the material has undertaken and will influence mechanical behaviour of the implant, therefore special attention must be given since the higher the corrosion rate, the sooner the mechanical integrity of the implant will be compromised.

Table 1: Corrosion rate values for Fe-based materials tested under Hanks solution environment. a) Electroformed iron; b) Equal Channel Angular Pressing iron

Sample	Corrosion rate (<i>mm/year</i>)	Reference
Cast iron	0,08	[5]
Annealed iron (550°C)	0,16	[22]
E-iron ^{a)}	0,85	[22]
ECAPed iron ^{b)}	0,02	[25]
Iron bar	0,11	[21]
Iron foam	0,75	[26]

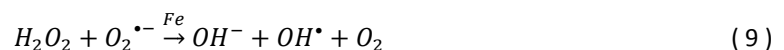
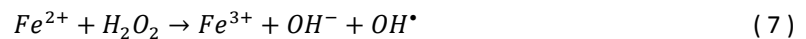
Finally, it is important to refer that degradation will also depend on the microstructure of the material, which is a consequence of the production process and surface treatment. Smaller grains will cause more susceptibility to corrosion due to larger numbers of grains and grain boundaries [7]. Also microstructural defects will contribute to a higher corrosion rate.

3.2 Toxicity of degradation products

Iron is present in the human body and participates in some biological activities like electron transfer and oxygen utilisation, which makes it crucial for the function of the body. In an average nutritional diet, the absorption of iron per day should be 1-2 mg, which is the quantity that corresponds to the loss of iron due to biological activity, and menstrual and other blood losses. As a result, the quantity of iron in a person is 35 and 45 mg/kg in an adult woman and man, respectively [14, 27].

Taken that into account, one may consider that in the presence of a biodegradable implant its corrosion products will not be toxic as long as the iron levels are kept under those critical values.

The toxicity of iron, when it is exposed to aerobic conditions, results from the Fenton and Haber-Weiss reactions [28]. In those reactions the production of free radicals, called ROI's (Reactive Oxygen Intermediates), causes damage to cells. This occurs naturally, because the metabolic process of producing radicals is a normal reaction in the body. However, the toxic part of radicals comes from the disrupted balance between these radicals and antioxidant defences, called oxidative stress. Antioxidants defences can regulate the activity of the radicals, preventing them from becoming harmful [28-30].



One may conclude that, when iron is in excess quantities in the body, the antioxidants are not sufficient to counter-balance the rapid production of radicals. As a consequence, the excess iron can cause, for instance, DNA damage and protein modification [30].

3.3 Interaction with cells

After looking into the possible toxicity of the iron released by the implant, it is important to consider the effect of iron in cells, since they are going to be exposed to a foreign material, and biological functions may be disturbed. This has been investigated by means of *in vitro* and *in vivo* studies carried out by several authors.

3.3.1 *In vitro* studies

Restenosis² is one of the problems that affect people with coronary stents. One solution to avoid this came from the use of iron as a biodegradable material, and so the relationship between corrosion product Fe(II) and smooth muscle cells (SMC) was investigated. These cells are produced as part of the healing process of the artery but, sometimes, its production does not stop after the healing occurs, and it accumulates in the artery causing restenosis and disturbing the blood flow. The presence of iron can cause a reduction in the metabolic process that produces those cells and thus contribute to avoid that effect.

Mueller et al. [31] verified that fact and the result of their study was that iron played a positive role in opposing the production of these cells by disturbing the regulatory gene expression of the cell cycle. Moreover, this result was confirmed by Moravej et al. [22] who noticed a decrease in the activity of SMC proliferation. In addition to that Nie et al. [25] not only verified the previous data, but also observed that the growth of endothelial cells and proliferation of fibroblast cells were promoted.

Blood compatibility studies performed by Zhang et al. [21] showed that iron has good anticoagulant properties, very close to those of stainless steel, and presents low surface adhesion of cells. The advantage of having these properties is the reduction of platelets around the implant, which in great density would increase the tendency for the occurrence of thrombosis.

The above studies indicated that iron shows good blood compatibility and, therefore, presents itself as a good candidate for implant applications in the medical field.

3.3.2 *In vivo* studies

There have been a few *in vivo* studies regarding biodegradable iron. The pioneer work in this field is from Peuster et al [19, 32]. In 2001 the authors published a study where the material was implanted in New Zealand white rabbits. The test results were evaluated six and eighteen months after the implantation and the goal was to determine if this material was safe to use as a cardiovascular implant. The results were very promising: there were no complications or adverse events within the period of implantation and the inflammatory response was minimal, which led to the conclusion that biodegradable iron could be safely used for this application.

On the other hand, it was verified that after one year, parts of the iron implant were still found in the site of implantation, which meant that the implant had not been totally degraded. Since then the

² Restenosis is the narrowing of a blood vessel.

need to enhance the degradation rate of iron implants has been highlighted in almost every study on the subject.

The same research team was engaged in another study, this time in a porcine descending aorta. The tests were conducted in 29 minipigs during a period of 360 days. The pigs showed no sign of iron toxicity in any of the animal organ or in the tissue around the implant. The conclusions confirmed those of the previous study about the safety of using Fe-based implants, however, the degradation rate of the material was again too slow.

More studies followed on this topic but all of them concerned only cardiovascular applications.

Waksman et al. [20] investigated the safety of a biodegradable iron implant, also in pigs, but instead of a long term, a short-period study was conducted (28 days). It was shown that after that period the implant was covered with a brownish layer of corrosion products, but there were no adverse effects related to this implant and its overall performance was good, showing once again that biodegradable iron stents are safe to use.

Mueller et al. [33] tested iron in a rat model, aiming to study the destination of corrosion products, gene expression in the implant and respective evaluation. It was concluded that this animal model might be more efficient in the initial state of a study and the results of previous studies were confirmed, such as limited tissue inflammation and slow degradation rate of iron.

Chao et al. [24] enrolled in a short-time study of 28 days in order to evaluate the safety and efficiency of biodegradable nitrided iron stents. Despite a slight difference in the material, compared to previous studies, the results also showed that it was safe; it was observed that in the degradation process the corrosion products did not cause any adverse effects.

In summary, all the *in vivo* experiments reported in the literature showed that iron has good biocompatibility and that the corrosion products are non-toxic. Implantation in animals showed no complications and the major problem encountered with these implants is the slow degradation rate, more specifically, the fact that parts of implanted iron are still present after one year of implantation. This clearly demonstrates that Fe-based materials have great potential as implant materials, provided that improvements are made to increase the degradation rate.

3.4 Mechanical properties

When an implant is placed in the body it needs to provide mechanical support to the damaged tissue while it is healing. After the healing process, mechanical strength of the implant should diminish in order for the healed tissue to assume the function of mechanical support. Meanwhile it is important to assure that the implant provides the necessary mechanical support before the surrounding tissue can take over its function.

Having that in mind, the mechanical properties of the implant should take into consideration the stresses that are applied to the damaged tissue and should be, as much as possible, similar to the tissue it is replacing. This is important, for example, in bone where stress shielding problems tend to occur when the implant has stiffness much higher than the bone tissue.

In cardiovascular applications, the arterial wall is exposed to a mechanical stress of 0,2-1 MPa, while in orthopaedic applications mechanical stress is 0-4 MPa for cancellous bone and 0-40 MPa for cortical bone [2].

Table 2: Mechanical properties of various materials. a) Electroformed Fe; b) Equal Channel Angular Pressure Fe

Material	Density (g/cm ³)	Yield strength (MPa)	UTS (MPa)	Young Modulus (GPa)	Elongation (%)	Reference
Cortical bone	1,8 - 2,0	105 - 114	35 - 283	5 - 23	-	[6]
Cancellous bone	1,0 - 1,4	-	1,5 - 38	0,01 – 1,57	-	[6]
SS316L	8,0	190	490	193	40	[2]
WE43 Mg alloy temper T6	1,84	170	220	44	2	[10]
Pure Fe	7,87	150	210	200	40	[2]
Annealed Fe (550°C)	-	140	200	-	25	[34]
E-Fe ^{a)}	-	270	290	-	18	[34]
ECAPed Fe ^{b)}	-	-	470	-	-	[25]

Mechanical properties of Fe show that an implant made of this material can withstand higher loads than Mg-based materials and thus, present higher potential for short-stay orthopaedic applications.

Furthermore, these properties can be improved with different production techniques and surface treatments. As shown in *Table 2*, E-Fe and ECAPed-Fe show enhanced mechanical properties. Different production techniques and optimized parameters will cause alterations in the microstructure. This also influences mechanical strength: finer microstructures with smaller grains usually correspond to higher mechanical resistance [7].

Iron has enough mechanical strength to withstand the stresses that cortical and cancellous bone are exposed to. However, one may think that because iron's stiffness is higher than that of natural bone it may lead to stress shielding effects. In fact, stress shielding is the protection of the bone from regular stresses that it is exposed to, leading to the reduction of the stimulation of the newly formed bone. For implants with extended stay in the body this may be a problem that can cause bone resorption and implant loss of adhesion, but in the case of biodegradable implants this will not be such a problematic issue because the mechanical integrity of the implant will decrease, which means that the growing bone will gradually be exposed to increased levels of stress and so a lack of stimulation of bone will not occur. However, attention should be paid since a slow degradation rate in the initial stage of the implant life in the body is expected and so the implant stiffness will always be higher than that of bone at that stage [4].

Additionally, mechanical properties of iron can further be improved by changing its microstructure. A finer microstructure could enhance mechanical properties. This is done either by choosing an adequate production method or a surface modification technique.

3.5 Production methods

There are several available production methods for biodegradable implants. The method is very important because it will determine the properties of the final implant. It influences microstructure, density, shape and much more. Therefore, special care must be taken when choosing the technique to use: if it is not chosen appropriately it will compromise the overall performance of the implant; it will influence not only mechanical but also the degradation properties.

The several techniques being used for the production of these materials include casting [7], powder metallurgy [35-41] and processes like electroforming [22, 34], 3D printing [42] and ECAP (Equal Channel Angular Pressing) [25].

In orthopaedic applications the presence of porosity in the implant is important since it promotes cell adhesion and bone growth [6]. A porous implant has also the advantage of degrading faster in the body than a dense implant. This aspect is relevant when choosing the production technique, since it is at this stage that porosity is created. Casting and ECAP can only produce dense components with no porosity, therefore, these methods are not suitable for porous implants.

Electroforming and 3D printing are layer-by-layer production techniques that allow rigorous control over dimensional parameters. However, electroforming needs a substrate that is removed afterwards, not producing bulk components. This comes as a disadvantage for this technique since for orthopaedic applications bulk pieces are required. 3D printing does not have that problem, but it is a time consuming technique and may not be adequate for mass production. In addition, it is also more expensive than powder metallurgy techniques.

A powder metallurgical route seems to be the most promising processing method in this area, not only because of the control provided over the porosity levels and because it can produce bulk components in a cost effective manner, but also because it is compatible with iron processing. In fact, the production of iron parts by powder metallurgy is well studied for other industries, such as the automotive [43]. In addition, optimised parameters such as applied pressure and thermal cycle in the sintering process can help achieving adequate mechanical and degradation properties.

3.5.1 Powder metallurgy

Powder metallurgy (PM) processes use a metal powder or a mixture of powders, followed by the respective compaction and sintering. If necessary, some optional manufacturing and finishing steps may be taken (*Figure 3*).

PM has the capability of producing components of materials that are not possible to produce with other fabrication techniques. In PM methods there is no liquid phase, which makes it adequate for materials with high melting points or for cases where solidification can compromise the material's chemical composition and properties. It has also the advantage of producing both dense and porous parts [43]. With this technique it is possible to obtain high density parts (up to 95% of dense material) [7].

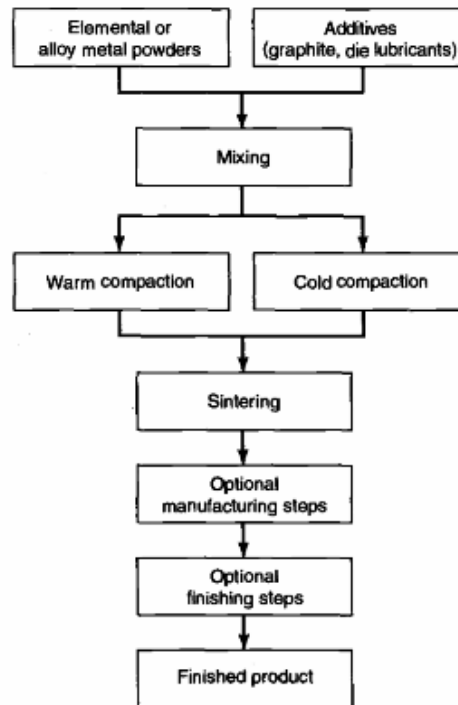


Figure 3: General steps of a PM process [38]

Despite that, the main challenges of PM techniques are the difficulties in producing very large components, to achieve high density levels and to control the grain sizes of materials. Parameters, such as sintering thermal cycle and raw material grain size, must be optimized in order to reach the desirable properties.

PM techniques include the conventional pressing and sintering processes, although there have also been reports on injection moulding used for this application. Other examples of PM techniques include powder forging, hot isostatic pressing, roll compaction, hot pressing and powder extrusion [35, 41].

3.5.2 Hot pressing technique

This technique involves pressing and heating at the same time. Heating combined with pressing is used to obtain high densification of the powder, which would not be possible with standard pressing at room temperature. It is a method typically used for ceramic materials, although it can also be used with metals or even for the production of composite materials.

Generally, the component is produced by inserting the powder into a die that is subjected to high pressure and heating, as described in *Figure 4*.

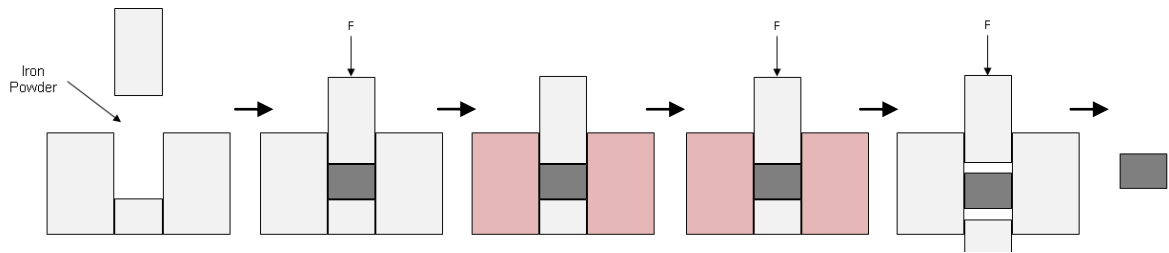


Figure 4: General steps of Hot Pressing technique: 1) Insert the powder in the die; 2) Apply a pre-pressure; 3) Heat the die, until the temperature stabilizes; 4) Apply pressure; 5) After cooling the sample is retrieved; 6) Final sample.

The exposure of the material to high temperature will lower its elastic limit, making it softer and easier to deform. In this way, compressibility is greatly improved and densification can be achieved through particle rearrangement, pore elimination and plastic deformation. With this technique it is possible not only to produce high strength parts, but also to allow a certain level of porosity, which is very important for a bone implant, since it promotes bone ingrowth [43-45].

4. Materials and Methods

This work concerned the preparation of porous Fe-based samples by hot pressing, followed by the respective characterization in terms of porosity, microstructure, mechanical properties and degradation behaviour as a function of the pressing parameters, and for different periods of immersion in a simulated body fluid solution.

4.1 Sample preparation

The samples were produced by hot pressing using a Carbonyl Iron powder (Iron 99,5 %, $D_{50}=5\mu\text{m}$) as starting material, shown in *Figure 5*.

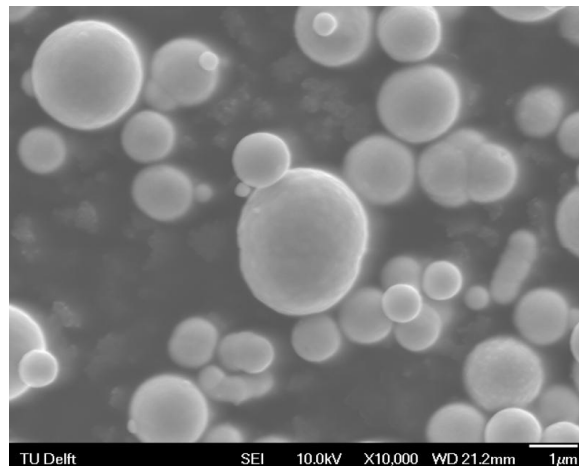


Figure 5: SEM image of iron powder

The hot press unit used for the experiments consisted of a conductive die surrounded by an induction coil, which generated heat by means of an electromagnetic field. This heat generation was independent of the applied pressure. The press used was a Carver M 3853 press equipped with heating plates (Carver M 2108.1). A Carver pellet die of 13 mm in diameter (model 3619) surrounded by a heating element Satec (1500 W) was used.

A zinc stearate lubricant was applied to the walls of the die in order to avoid friction related problems. Hot pressing was carried out at a constant pressure of 100 MPa. With the aim of assessing the influence of temperature on the level of porosity achieved in the samples, three different processing temperatures were used: 100 °C, 200 °C and 400 °C.

The hot pressing cycle consisted of heating the die to the desired temperature at a rate of 10°C per minute, followed by a period of 15 minutes for temperature stabilization. After that a uniaxial pressure was applied for one hour, followed by a cooling step.

The shape and size of the samples obtained are presented in *Figure 6*.

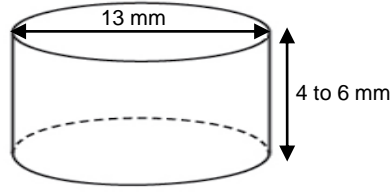


Figure 6: Schematic of sample shape and sizes after hot pressing

4.2 Porosity measurements

The bulk porosity and the surface porosity of the samples were determined.

The bulk porosity was determined by using Eq. 11 [46], from experimental measurements of density (Eq. 10).

$$\rho_{exp} = \frac{m}{V} \text{ (g/cm}^3\text{)} \quad (10)$$

$$Porosity (\%) = 1 - \frac{\rho_{exp}}{\rho_{Theoretical}} \quad (11)$$

ρ_{exp} – experimental density

$\rho_{theoretical}$ – theoretical density of iron (7,874 g/cm³)

Three samples produced at each processing temperature were tested and for each sample three measurements were made. Experimental density was determined from measurements of the mass of the samples and the respective volume by liquid displacement during immersion in water.

In order to determine surface porosity, the standard test method for oil impregnation was used as described in ASTM B963-3 [47]. Although this standard deals with the determination of interconnected porosity, in the case of the samples tested it was possible to determine surface porosity because these samples had closed porosity.

The numbers of samples and measurements performed were the same as those for the bulk porosity test and, the surface porosity was obtained using the following equation [47]:

$$Porosity (\%) = \left(\frac{B-A}{(B-F) \times \rho_{oil}} \times 100 \right) \times \rho_{water} \quad (12)$$

B – Mass of oil-impregnated sample (g)

A – Mass of oil-free/dry sample (g)

F – Mass of oil-impregnated sample dipped in water (g)

ρ_{oil} – Density of oil (g/cm³)

ρ_{water} – Density of water (g/cm³)

4.3 Static corrosion tests

The degradation of porous samples was assessed by static immersion and electrochemical corrosion tests.

The samples for static immersion tests were mounted in epoxy resin, mechanically polished with SiC papers from 800 to 1200 grit, followed by cleaning with ethanol. The static immersion tests were performed by immersing the samples in Hank's balanced salt solution (Sigma H1387), whose composition is shown in *Table 3*. A buffer was added, in order to maintain a pH value of 7.4. The tests were carried out at a constant temperature of 37.5 °C.

Table 3: Composition of Hank's Balanced Salt Solution

Component	CaCl ₂ ·2H ₂ O	MgSO ₄ (anhydrous)	KCl	KH ₂ PO ₄ (anhydrous)	NaCl	Na ₂ HPO ₄ (anhydrous)	D- Glucose	NaHCO ₃
Concentration (g/L)	0,185	0,09767	0,4	0,06	8	0,04788	1	0,35

Three batches of samples were prepared, each containing three samples from each of the three different temperatures used (100 °C, 200 °C and 400 °C). The first batch of samples was immersed for 7 days, the second one for 15 days and the last one for 30 days. After the tests, the samples were taken out of the bath and dried at room temperature. Note that for the purpose of this work, the immersion tests were meant for the determination of the corrosion mechanisms of the iron samples. For a complete assessment of the material behaviour in the human body longer test periods are required.

4.4 Electrochemical corrosion tests

Electrochemical corrosion tests were performed under the same condition as in the static corrosion tests (the same solution, pH and temperature), using a 3 electrode cell with platinum as the auxiliary electrode and calomel as the reference electrode.

For the electrochemical corrosion tests two samples were used: 200 °C and 400 °C. The samples were, previously mounted in epoxy resin, polished and spot welded to a conductive wire. The exposed surface area was 1 cm².

Potentiodynamic curves were plotted from -0.5 to 0.5 V, at a scanning rate of 0,166 mV/s. The corrosion potential and corrosion rate were determined using the Tafel extrapolation method. In addition, open circuit potential curves were determined over a period of one hour and recording one point per second. These two curves constituted one cycle and the sample of 400 °C was exposed to three cycles and the 200 °C to two.

4.5 Diametrical compression tests

Mechanical degradation of the samples was evaluated by diametrical compression tests, also called “brazilian disc tests”. This type of tests was used due to, not only the geometry of the sample, but also due to its extensive use to determine the strength in powder compacted materials [48-50].

The tests were performed on samples produced at different temperatures, both in the as-pressed condition and after the static immersion tests for 7, 15 and 30 days. A load cell of 10 kN was used, and the configuration of the sample and holders is shown in *Figure 7*. The tests were carried out according to the ASTM D3967-08 standard [51].

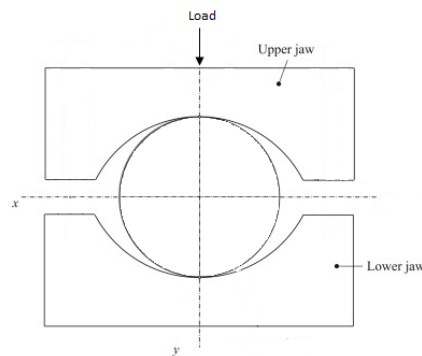


Figure 7: Schematic illustration of the configuration of sample and holders for the diametrical compression tests

The cylindrical samples were placed in contact with the lower and the upper jaws. The lower jaw was fixed and a load was applied through the upper one. Accordingly, a compression force was applied on the side of the sample, along its diameter.

The compressive load applied induced a tensile stress perpendicular to the applied load that causes fracture. The splitting tensile strength (σ_t) was calculated assuming the crack initiated at the point of the maximum tensile stress, according to *Eq. 13* [51].

$$\sigma_t = \frac{2P}{\pi LD} \quad (13)$$

P - Maximum applied load (N)

L - Thickness of the specimen (mm)

D - Diameter of the specimen (mm)

4.6 Microstructural characterization

The characterization of the microstructure of the samples prepared at different temperatures before and after the immersion corrosion tests for different times (0, 7, 15 and 30 days), was made by scanning electron microscopy (SEM) and x-ray energy dispersive spectrometry (EDS). The scanning electron microscope used was a JEOL JSM-6500F, combined with an EDS spectrometer INCA Energy, Oxford Instruments. This also allowed the identification of the corrosion products formed at the surface, contributing to an understanding of the degradation mechanisms occurring in these samples.

5. Results

5.1 As-pressed samples characterization

5.1.1 Microstructure

SEM images of the as-pressed samples are presented in *Figure 8* for the different processing temperatures used.

The sample pressed at 100 °C shows a regular arrangement of undeformed and apparently unreacted powder particles (*Figure 8 a*). One can clearly see the spherical shape and sizes of iron powder particles, indicating that the samples did not experience plastic deformation or interaction with each other during the processing stage at this temperature.

On the contrary, the microstructures of the samples pressed at higher temperatures (200 °C and 400 °C) clearly show interconnections developed between powder particles, forming a porous network structure where only some of very small original powder particles can be distinguished (*Figure 8 b and c*). The microstructures indicate that sintering of powder particles occurred at these temperatures with the formation of bonds between particles, which was not observed in the samples produced at the lower temperature.

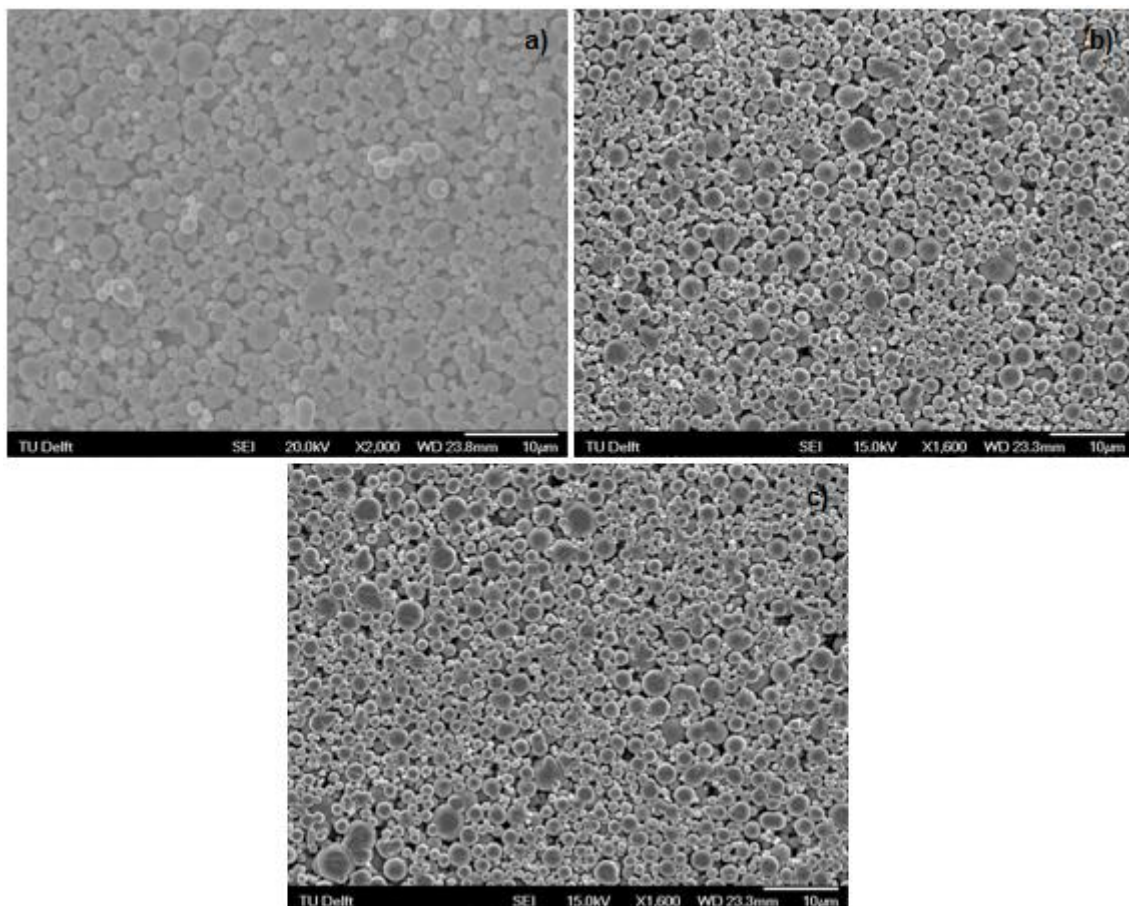
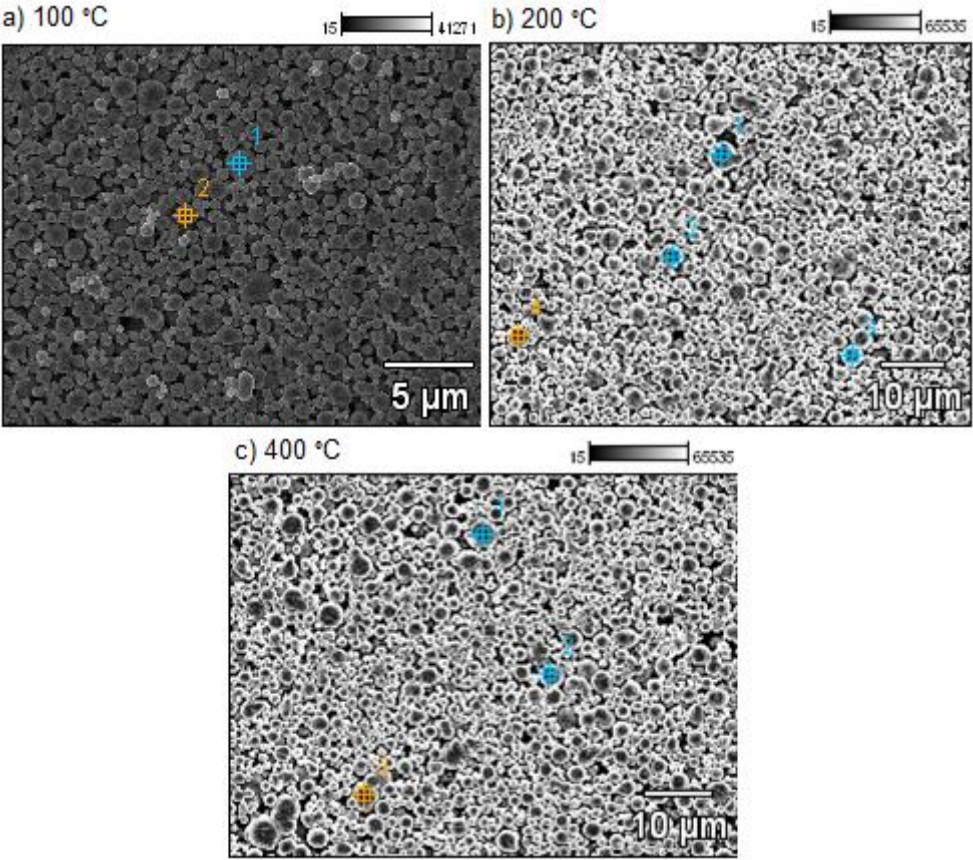


Figure 8: SEM micrographs of samples pressed at a) 100 °C, b) 200 °C and c) 400 °C

EDS microanalysis on the as-pressed samples shows that the only element present in the surface layer of the samples is iron with traces of carbon, confirming that there was no contamination of the material during the pressing process (Figure 9).



	Compound (wt%)	C	Fe
a) 100 °C	Point 1	-	-
	Point 2	-	100.00
b) 200 °C	Point 1	1.77	98.23
	Point 2	1.08	98.92
	Point 3	-	100.00
	Point 4	-	100.00
c) 400 °C	Point 1	1.68	98.32
	Point 2	-	100.00
	Point 3	-	100.00

Figure 9: EDS results of the as-pressed samples

5.1.2 Porosity

After pressing, the bulk density was measured in order to determine the amount of porosity present in the samples as a function of the pressing temperature.

These values are presented in *Figure 10*. There are no significant differences in porosity between the samples pressed at 100 °C and 200 °C, which present an average porosity of 56%. However, there is an obvious decrease in porosity in the samples pressed at 400 °C (39%).

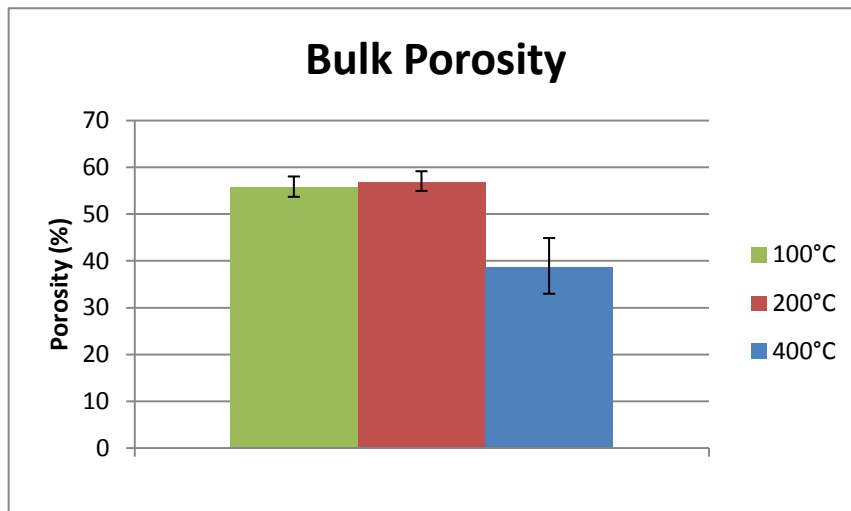


Figure 10: Bulk porosity of samples produced by hot pressing at different temperatures.

As expected, the samples pressed at higher temperature (400 °C) showed less porosity than those pressed at lower temperatures. This is because, at higher temperatures, the material softens, making it easier for the powder to deform, and so pressing will increase the contact between powder particles and reduce the porosity [45].

In terms of surface porosity, the samples produced at 100 °C and 200 °C present values of 2,8 - 3%, while that pressed at 400 °C presents a slightly lower value of surface porosity (2,3%) (*Figure 11*).

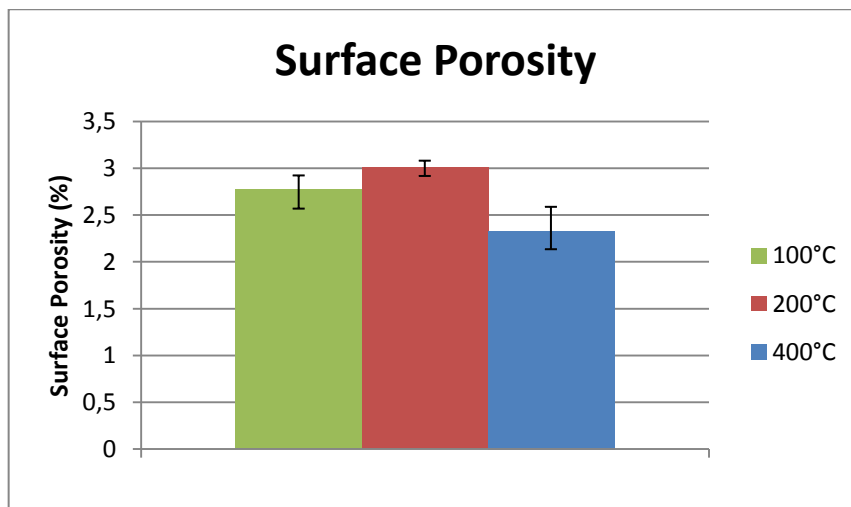


Figure 11: Surface porosity of samples produced by hot pressing at different temperatures.

5.1.3 Electrochemical behaviour

Open circuit potential curves for the samples processed at 200 °C and 400 °C are presented in *Figures 12 and 13*, respectively. (The sample processed at 100°C was not used in this experiment due to its high level of porosity, which is inappropriate for this technique).

The curves show a rapid decrease of potential in the first stage that then the corrosion potential value tends to stabilise.

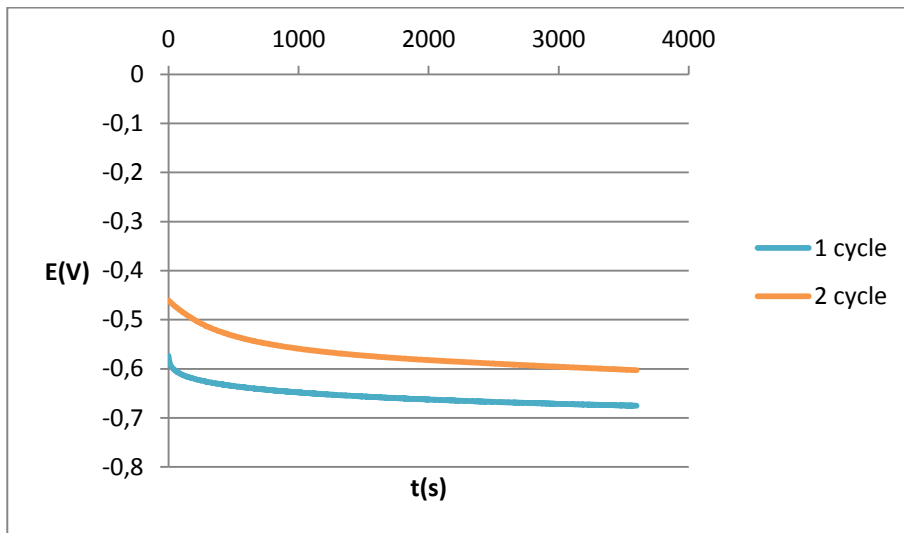


Figure 12: Open potential curves of samples pressed at 200 °C

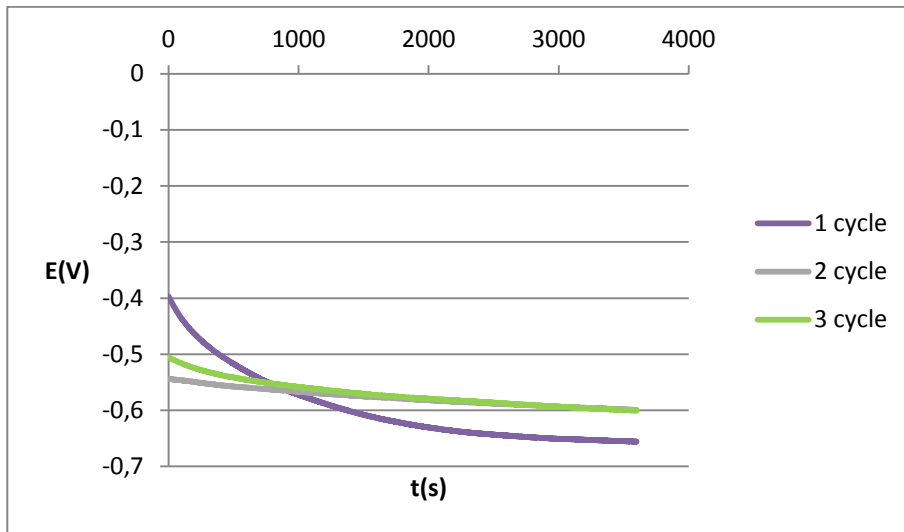


Figure 13: Open potential curves of samples pressed at 400 °C

The potentiodynamic curves obtained for the samples pressed at 200 °C and 400 °C are presented in *Figures 14 and 15*, respectively. The curves show the cathodic (*Eq. 2*) and anodic (*Eq. 1*) reactions occurring at the surface of the metal. The cathodic reaction corresponds to the decreasing curve (the lower part of the curve), while the anodic one corresponds to the increasing curve (the upper part of the curve). When the behaviour changes from anodic to cathodic the corrosion current and potential are extrapolated and the corrosion rate can be calculated. This corrosion potential should match the value of the corrosion potential of the respective open circuit potential curves.

However, this is not verified by the results presented in this work. In fact, the results show that the potentiodynamic corrosion potential is lower than the one observed in the open circuit curve. This can be explained by a local increase of pH close to the surface of the sample, since corrosion potential is strongly influenced by the pH of the solution.

On the other hand, the change in pH also causes the formation of a passive film, which can be detected in the slope of the anodic curve in all the samples tested. After passivation of the metal the corrosion is dominated by pitting (non-uniform corrosion), which is not wanted. Despite that, it is still possible to determine the corrosion potential by means of the cathodic curve, and so the Tafel extrapolation method was still used to determine not only that, but also the corrosion current and the corrosion rate of the samples tested. The results are presented in *Table 4*.

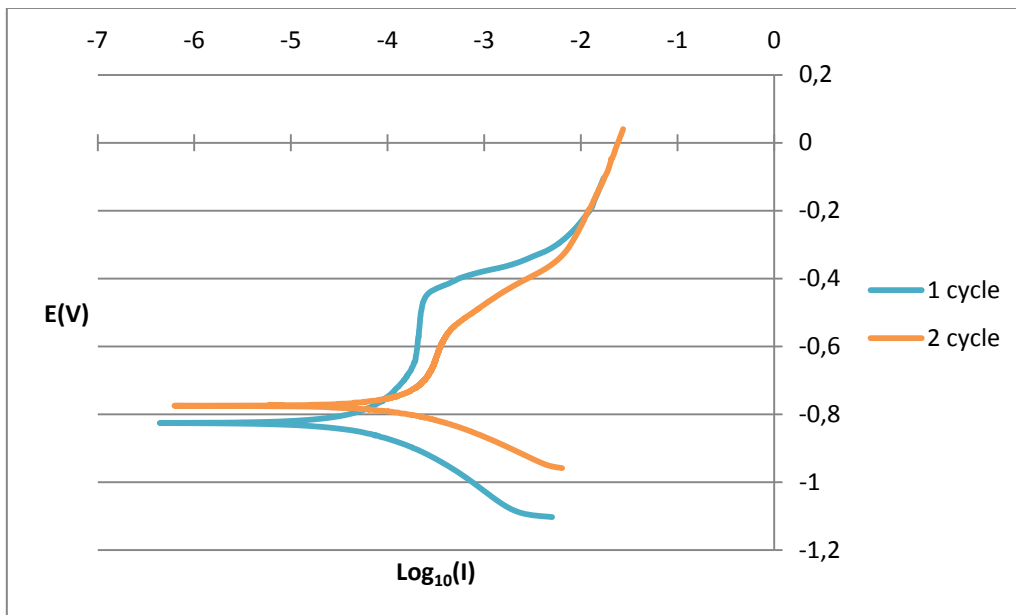


Figure 14: Potentiodynamic curves of samples pressed at 200 °C

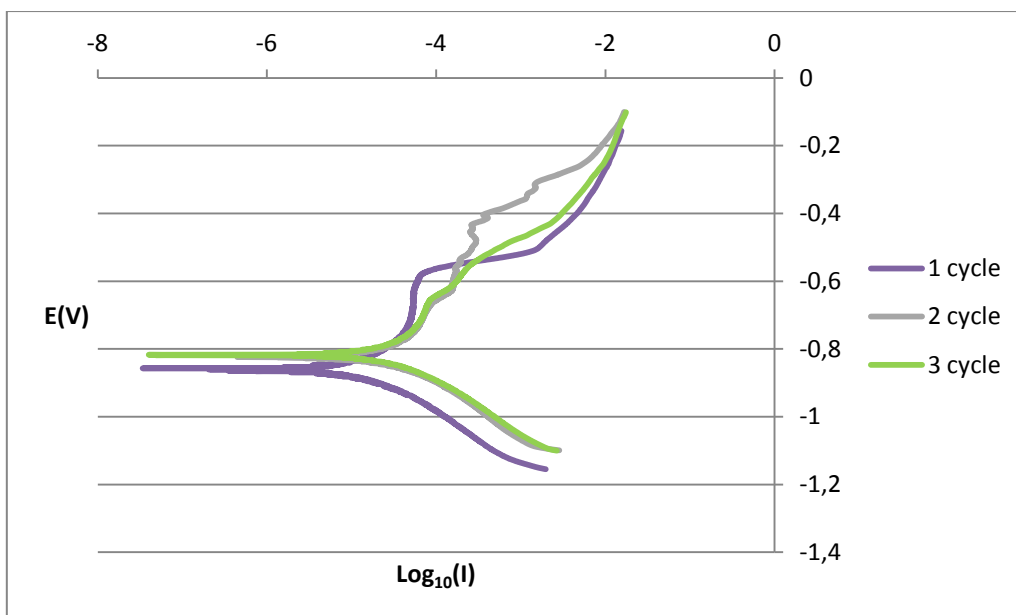


Figure 15: Potentiodynamic curves of samples pressed at 400 °C

Table 4: Results of the Tafel extrapolation method

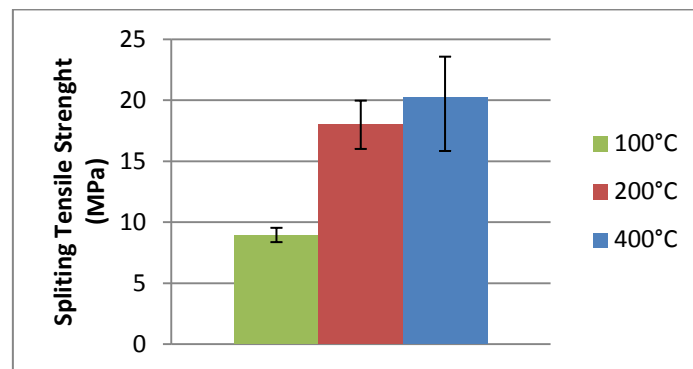
	E_{corr} (V)	i_{corr} ($\mu A/cm^2$)	Corrosion Rate (mm/year)
400°C	-0,863	0,194	0,222
	-0,824	0,428	0,490
	-0,819	0,407	0,465
200°C	-0,770	0,017	1,927
	-0,825	0,881	1,009

From *Table 4*, it is possible to observe that the average values of the corrosion potential and current and the corrosion rate are higher for the samples pressed at 200 °C than for those processed at 400 °C. This happens because the samples pressed at 200 °C have higher porosity, which means that they have a larger surface area exposed to the corrosion medium. An enlarged corrosion area will make it easier for the medium to attack the samples and so, the corrosion rate will be higher.

One can also notice that the difference in the corrosion potential values between the first and second cycles is significant. In fact, all the samples tested showed an increase in this value, meaning that there is a decrease in corrosion resistivity in the second cycle. This happens because the air in contact with the samples formed an oxide film on the surface, which constituted a protective layer against corrosion. After the first cycle that barrier was broken, making it easier for the metal to corrode in the following cycles [26, 36].

5.1.4 Mechanical behaviour

The results of the compression tests in the as-pressed samples are presented in *Figure 16*.

**Figure 16: As-pressed samples' compression results**

Bonding between particles will make the material stronger and so, the higher the processing temperature, the higher strength the material will have [49]. In *Figure 16* the increasing strength of the material with increasing temperature is obvious.

It is clear that the samples pressed at 200 °C and 400 °C present a splitting strength about twice higher (18-20 MPa) than that produced at 100 °C (9 MPa). This is surely related to the microstructure of the samples produced at different temperatures (see *Figure 8*), where it was clearly observed that only the samples produced at 200 °C and 400 °C developed structures with interconnectivity between powder particles.

5.2 Characterization of samples after immersion tests

5.2.1 Microstructure

The surfaces of the samples after the immersion tests were studied by using SEM and EDS. In *Figure 17* images of the surfaces of the samples produced at 100 °C before and after immersion for different periods are presented.

The images show the corrosion products formed on the surface of the samples during immersion. After 7 days of immersion, a structure consisting of elongated particles was formed, which covered most of the samples' surface (*Figure 17 b*), and seemed to indicate a directional growth. In the sample immersed for 30 days, the surface is covered with small aggregates of particles with a powdery shape showing no specific orientation (*Figure 17 c*).

The results of EDS analysis of the corrosion products formed on the surface of the samples pressed at 100 °C after immersion are shown in *Figure 18*. The corrosion products formed after immersion contain mainly oxygen and iron in their constitution, suggesting the formation of iron oxide.

After 7 days of immersion, phosphorous, chlorine and calcium are also present on the surface of the samples, which suggests that Hank's solution compounds precipitated (*Figure 18 a*). The elongated particles observed in SEM contained iron, oxygen, phosphorus and calcium.

On the samples immersed for 30 days (*Figure 18 b*) the presence of phosphorous and calcium is accentuated, however, chlorine was not detected on the surface of the sample. The presence of increased amounts of phosphorous and calcium in the sample immersed for 30 days suggests the formation of some form of calcium phosphate, that typically occurs in metal after immersion for long periods in Hank's solution [52-54].

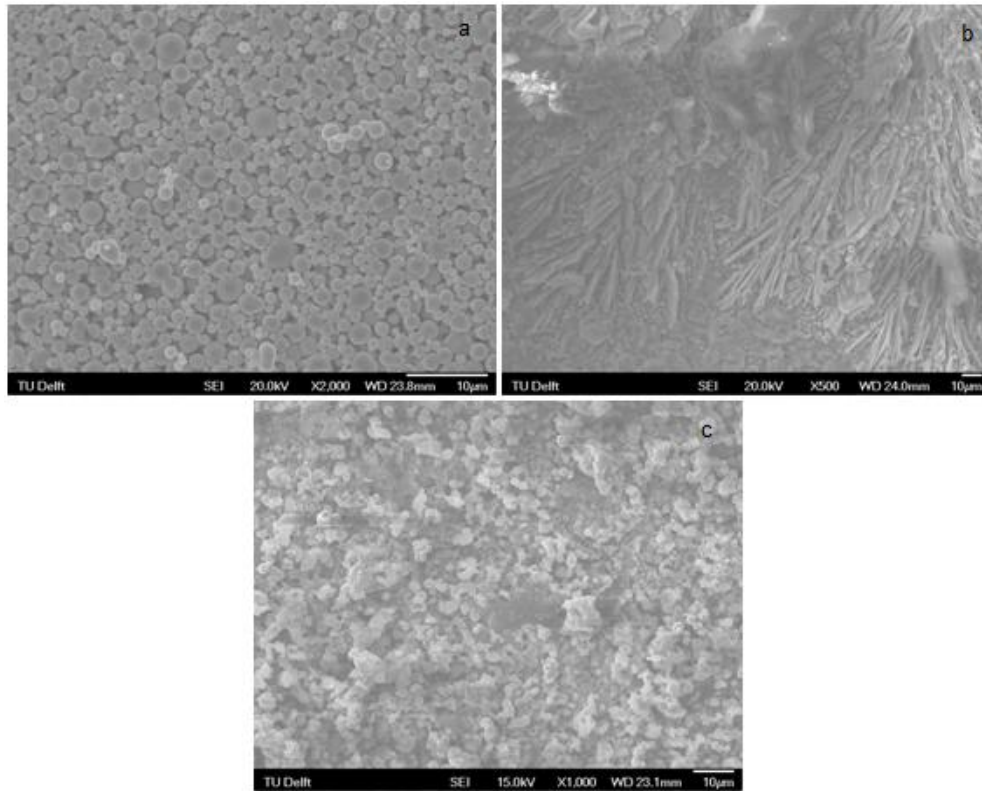
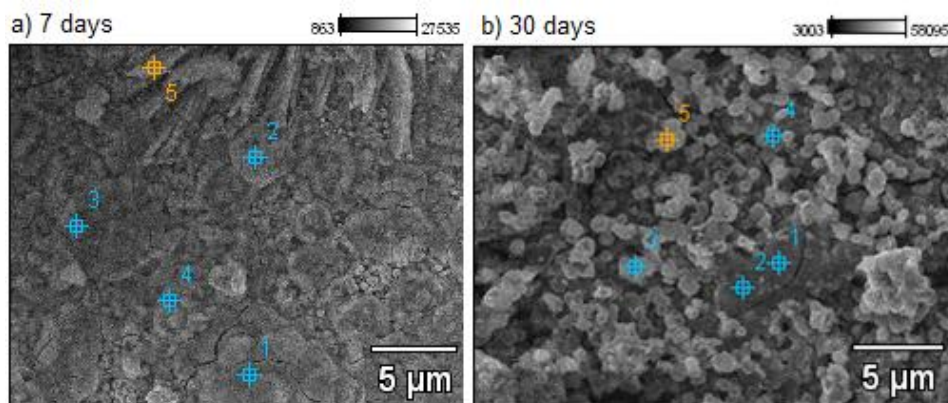


Figure 17: SEM images of iron processed at 100 °C: a) as-pressed; b) after immersion for 7 days; c) after immersion for 30 days.



	Compound (wt%)	C	O	P	Cl	Ca	Fe
a) 7 days	Point 1	-	46.69	-	-	-	53.31
	Point 2	-	36.16	-	26.17	-	37.68
	Point 3	1.49	46.98	-	-	-	51.53
	Point 4	-	38.94	-	-	-	61.06
	Point 5	-	44.01	23.16	-	4.45	28.38
b) 30 days	Point 1	-	33.28	4.65	-	8.24	53.83
	Point 2	-	39.56	6.36	-	10.86	43.22
	Point 3	2.24	36.52	4.58	-	6.71	49.95
	Point 4	-	31.47	-	-	-	68.53
	Point 5	2.24	39.11	7.06	-	13.21	38.37

Figure 18: EDS analysis results of a sample pressed at 100 °C after different immersion periods

Concerning the samples pressed at 200°C (*Figure 19*), the formation of directional structures on the surface was also observed. These structures are observed in samples immersed for 7 and 15 days (*Figure 19 b and c*). However, the morphology of the precipitates formed at the surface of the sample immersed for 30 days changes to aggregates of particles with a powdery shape, similar to those observed in the 100 °C sample immersed for the same period (*Figure 19 d*).

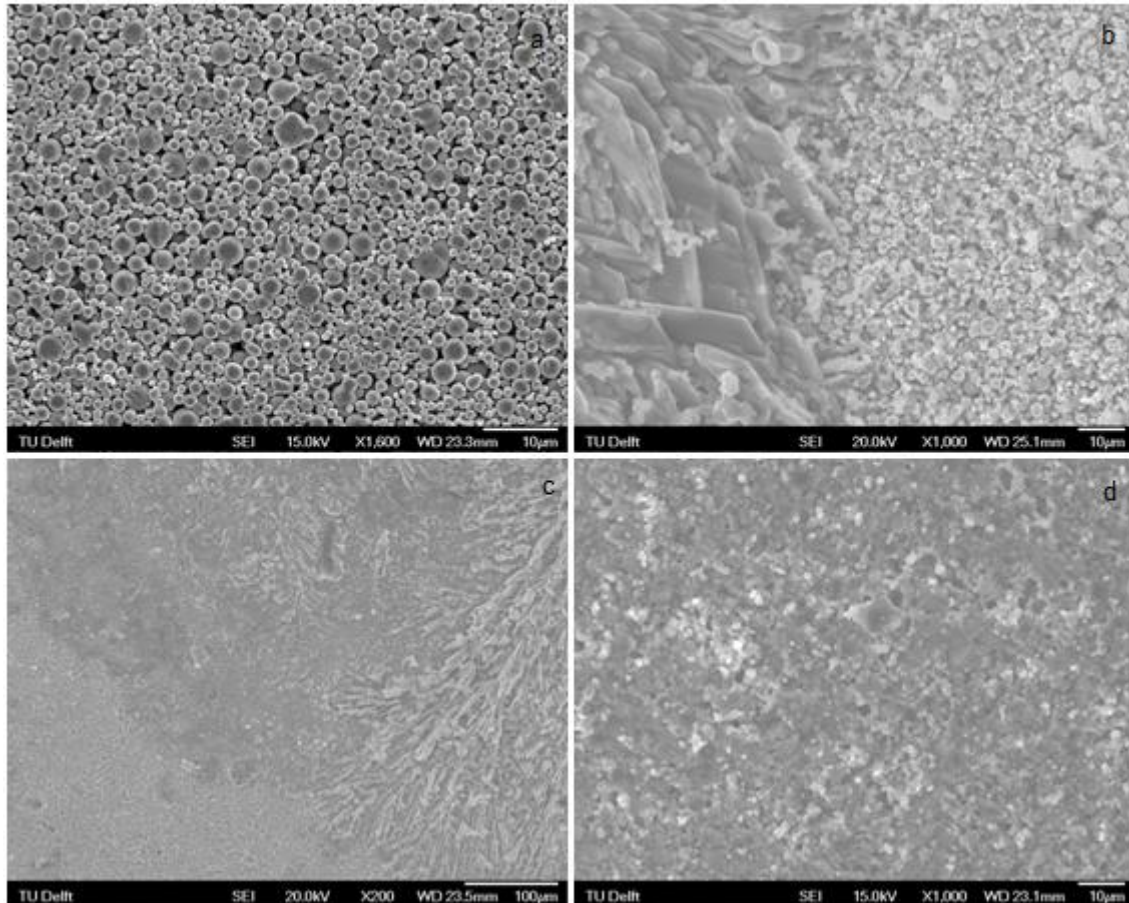


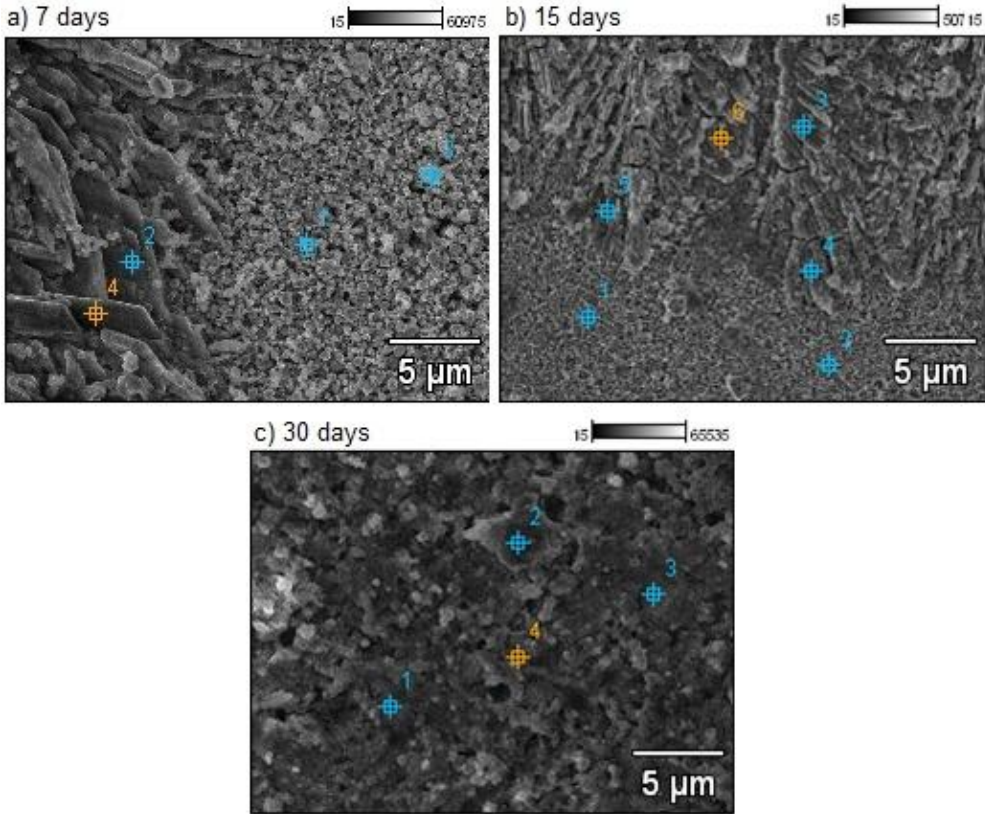
Figure 19: SEM images of iron processed at 200 °C: a) as-pressed; b) after immersion for 7 days; c) after immersion for 15 days; d) after immersion for 30 days.

EDS analysis of the samples pressed at 200 °C also showed the presence of iron and oxygen in all the time points. On the samples immersed for 7 days, the presence of carbon, and phosphorous was observed (*Figure 20 a*). In the elongated particles on the surface, iron, oxygen and phosphorous were the elements present.

After 15 days of immersion the same elements are present on the surface of the samples, and evidence of other elements, namely sodium, potassium and calcium was also found (*Figure 20 b*).

On the samples immersed for 30 days (*Figure 20 c*), the same elements were present, as in the samples collected after 15 days of immersion, with the exception of potassium, that was absent in these samples. As in the previous sample (100 °C) there is an increase amount of phosphorous and calcium in the precipitates formed at higher immersion periods, suggesting the formation of increased amounts of calcium phosphate particles.

It is clear that, on one hand, these precipitates result from the oxidation of iron and, on the other, from particles (calcium phosphates) deposited from the Hank's solution. This is consistent with the results from the samples pressed at 100 °C, which showed similar elements on the surface. The samples pressed at 100 °C after 7 days of immersion showed similar elements as the samples pressed at 200 °C after 15 days of immersion, suggesting that the same corrosion mechanisms occurred on the surface of these samples, but at an accelerated corrosion rate.



	Compound (wt%)	C	O	Na	P	K	Ca	Fe
a) 7 days	Point 1	8.05	-	-	-	-	-	91.95
	Point 2	-	50.74	-	22.06	-	-	27.20
	Point 3	3.83	3.13	-	1.36	-	-	91.68
	Point 4	-	37.85	-	49.24	-	-	12.91
b) 15 days	Point 1	-	12.81	0.91	-	-	-	86.28
	Point 2	3.15	22.35	1.68	6.52	-	-	66.30
	Point 3	-	37.04	1.92	14.00	5.05	22.56	19.43
	Point 4	2.14	41.03	2.25	10.13	-	16.66	27.80
	Point 5	-	39.64	2.21	10.41	-	16.05	31.69
	Point 6	1.59	41.01	1.73	11.55	2.61	15.86	25.65
c) 30 days	Point 1	6.03	39.19	2.01	17.11	-	15.99	19.67
	Point 2	3.25	36.90	-	22.03	-	15.67	22.15
	Point 3	2.19	16.74	-	6.27	-	11.88	62.92
	Point 4	6.53	40.70	-	25.35	-	5.05	22.37

Figure 20: EDS analysis results of a sample pressed at 200 °C after different immersion periods

The images obtained from the samples processed at 400 °C (*Figure 21*) also showed formation of corrosion products on the surface. However, the morphology of the structures formed is different from that in the previous samples. After 7 days of immersion, the surface was covered with a dense layer of relatively small equiaxed particles (*Figure 21 b*). After 15 days of immersion, large hedgehog-like structures were present on the surface (*Figure 21 c*), that after 30 days of immersion tend to develop into fully grown columns, forming a rough layer that covered the entire surface (*Figure 21 d*).

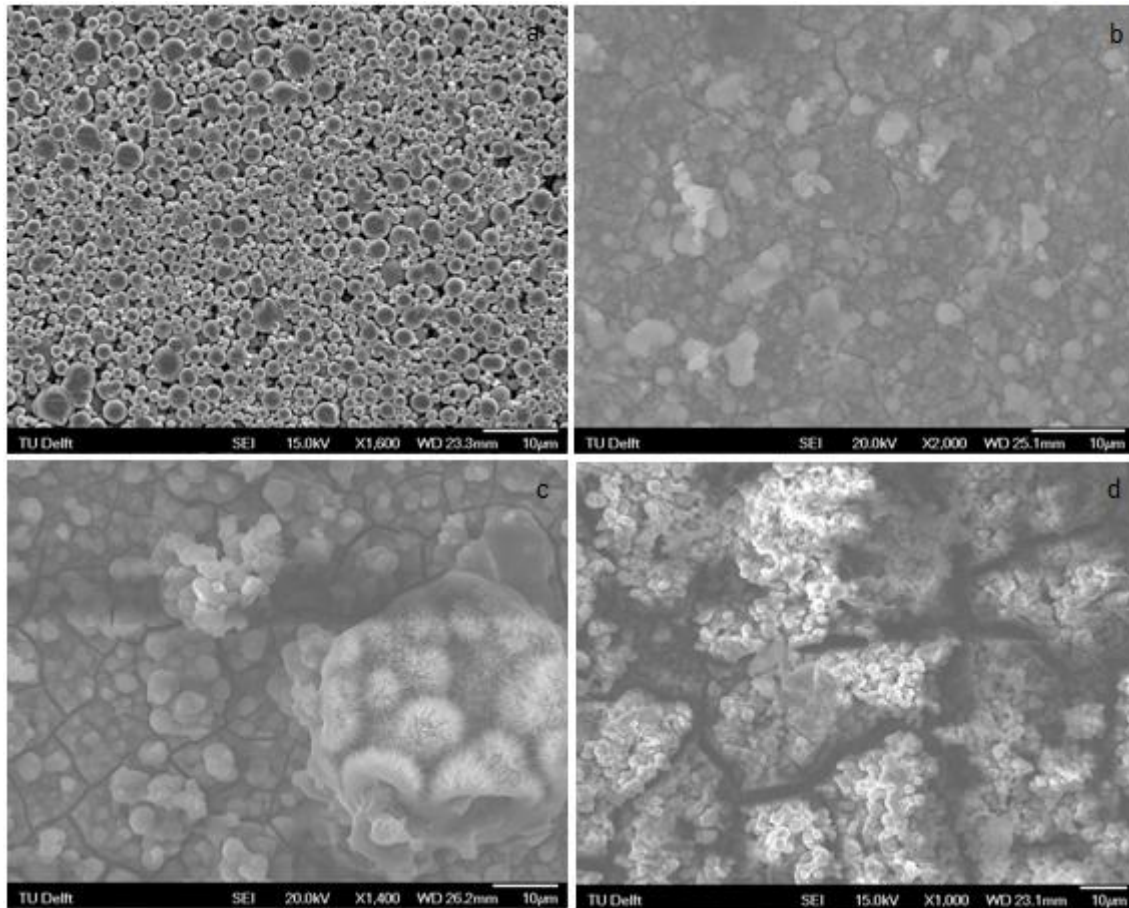
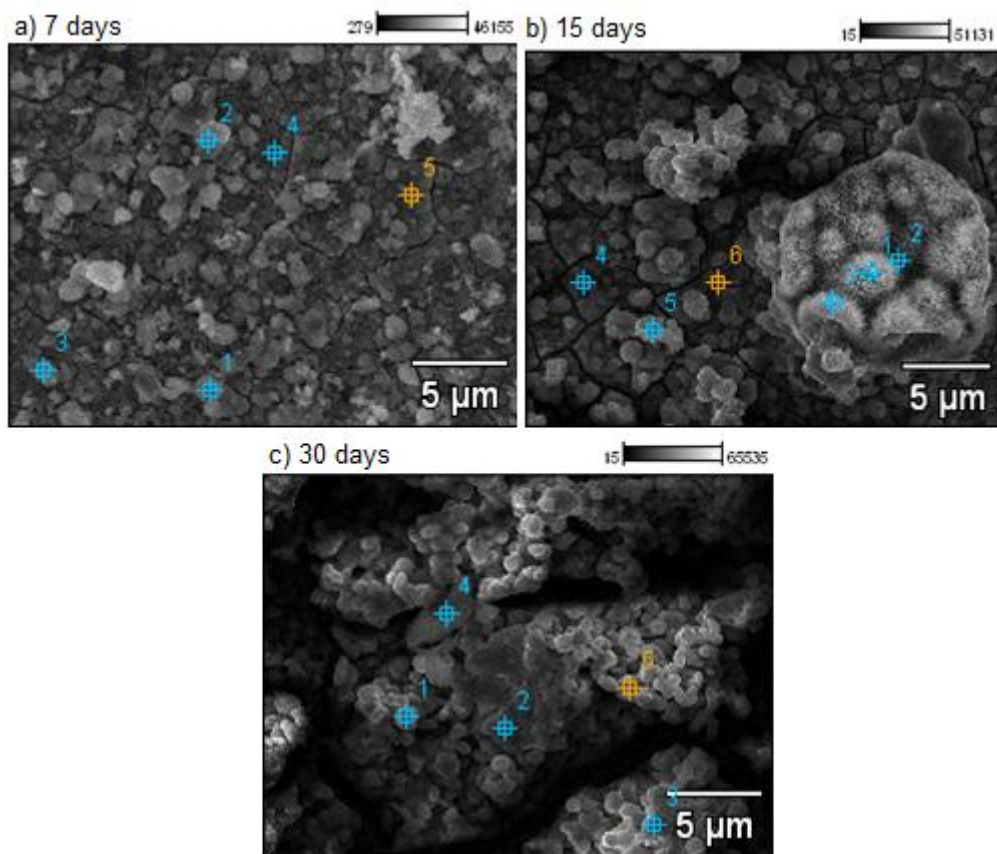


Figure 21: SEM images of iron processed at 400 °C: a) as-pressed; b) after immersion for 7 days; c) after immersion for 15 days; d) after immersion for 30 days.

Figure 22 presents the results of the EDS analysis of the samples processed at 400 °C after the different immersion periods. After 7 days of immersion the corrosion products contained carbon, oxygen, sodium, phosphorous, potassium, calcium and iron in their constitution (*Figure 22 a*). This composition suggests the formation of a more complex precipitate or mixture of precipitates, containing probably calcium and iron phosphates, carbonates and oxides. However, the main difference to the previous samples is the presence of calcium and phosphorous, also after immersion for 7 days, which suggests a higher bioactivity of the current sample surface and probably a different corrosion mechanism.

After immersion for 15 and 30 days (*Figure 22 b and c*), the same elements as in the previous processing temperatures were present on the surfaces of the samples, suggesting a regular mechanism of corrosion in this material for the different immersion periods.



	Compound (wt%)	C	O	Na	P	Cl	K	Ca	Fe
a) 7 days	Point 1	2.80	40.07	3.10	16.47	-	1.97	11.79	23.81
	Point 2	-	35.75	2.12	21.09	-	2.81	19.30	18.93
	Point 3	-	33.14	2.46	28.22	-	-	22.96	13.21
	Point 4	-	35.55	2.46	20.92	-	-	21.19	19.88
	Point 5	-	40.81	2.66	20.29	-	4.25	18.19	13.81
b) 15 days	Point 1	-	39.84	-	-	18.36	-	3.62	38.18
	Point 2	-	32.92	-	-	26.76	-	-	40.32
	Point 3	-	41.59	-	1.69	24.16	-	-	32.56
	Point 4	-	35.18	1.50	25.19	-	3.40	21.33	13.40
	Point 5	1.34	37.77	1.40	24.17	-	3.33	20.99	11.00
	Point 6	1.30	26.80	-	27.16	-	6.22	26.73	11.79
c) 30 days	Point 1	4.22	38.25	2.44	13.15	-	-	11.16	30.77
	Point 2	3.58	43.19	2.41	14.39	-	2.44	10.02	23.97
	Point 3	8.77	32.52	-	13.98	-	-	13.76	30.97
	Point 4	39.67	29.88	-	6.28	-	-	5.43	18.74
	Point 5	4.43	39.96	2.55	12.96	-	2.43	7.44	30.23

Figure 22: EDS analysis results of a sample pressed at 400 °C after different immersion periods

5.2.2 Mechanical behaviour

The results of the compression tests in the samples subjected to the immersion tests are presented in *Figure 23* along with the results from the as-pressed samples (corresponding to 0 days) for comparison.

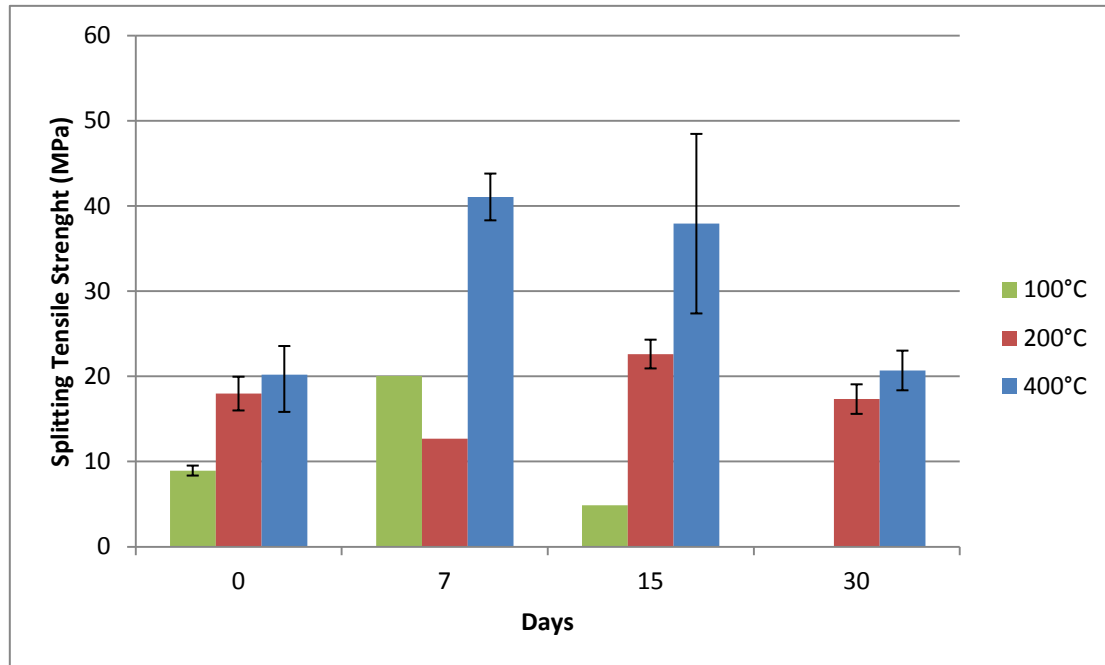


Figure 23: Results of diametrical compression tests

The samples pressed at 100 °C show a slight increase in mechanical strength after 7 days of immersion, but after longer immersion times its resistance decreases again. The sample immersed for 30 days disintegrated even before the compression test and that is why it was not possible to test.

Regarding the samples produced at 200 °C, the mechanical test results presented no significant variation in their mechanical strength after immersion for different periods of time. There is a slight decrease in strength after 7 days of immersion that then increases after immersion for longer periods to values closed to the as-pressed material.

On the other hand, the samples processed at 400 °C showed a considerable increase in strength after immersion for 7-15 days. The splitting strength reached a level of about 40 MPa, which suggests that reactions occurred on the surface of the material that caused the formation of molecules that have a binding role in the structure and contributed to these increased values of strength. However, immersion for a longer period of 30 days caused a decrease in strength, to the level of the as-pressed sample (20 MPa). This decrease should be expected due to increased exposure of the material to the corrosion medium.

6. Discussion

The results of as-pressed iron showed that different levels of porosity are possible to obtain in an iron-based material, using different processing temperatures, and the level of porosity decreases with increasing temperature due to increasing sinterability with this parameter.

Hot pressing at 100 °C does not promote significant densification or consolidation of the material, however, pressing at temperatures of 200 °C and 400 °C causes an increase in the density of the samples, because exposure to higher temperatures softens the material, making it easier to deform by compression forces. At higher temperatures solid diffusion processes at the particles interface are enhanced, promoting bonding [45].

SEM images, along with electrochemical and mechanical tests seem to support this argument. In fact, the samples tested showed increasing strength with increasing processing temperature, since particles are more strongly bonded when pressed at higher temperature.

However, upon comparison with other studies conducted on this topic one can see that the initial strength of this material is too low. For the higher processing temperatures, the results obtained, showed a strength of 20 MPa and materials currently used for short-stay orthopaedic devices in the body present a minimum strength of 200 MPa [2, 6, 10, 25, 34]. Even when compared to the strength of the human bone, the values obtained in this work do not reach the strength necessary for an application in the cortical bone [2], which makes this material inappropriate for orthopaedic applications, in terms of mechanical properties. Sintering at higher temperature or a low degree of porosity would probably be necessary to obtain a material with the level of strength necessary for an orthopaedic application.

In what concerns the corrosion properties, the presence of porosity greatly increased the corrosion rate of the material. For the material processed at 400 °C, the results obtained are similar to the highest values for biodegradable iron found in the literature [22, 26]. As for the samples pressed at 200 °C, the results obtained doubled the ones obtained previously. These results show that the corrosion rate was definitely improved.

However, when one combines the corrosion rates with the mechanical properties obtained in the materials developed in the present study, it is possible to conclude that, despite the good values obtained in terms of degradation, the mechanical properties were compromised and do not fulfil the requirements for orthopaedic devices.

The analysis of the precipitates formed on the surface of the iron samples after immersion suggests that two phenomena occurred: corrosion of the material with the formation of oxides and/or hydroxides; deposition of calcium and/or iron phosphates.

The deposition of calcium phosphates occurs typically in materials submitted to long-term immersion in Hank's solution [52-54].

Both phenomena seem to be occurring in all the tested samples but at different levels of intensity. In the samples pressed at 100 °C and 200 °C for short period (7 days), mainly the formation

of iron oxides/hydroxides occurs, with very little expression of phosphates formation (an Fe phosphate may form) [21]. Those precipitates didn't seem to affect the mechanical properties of the material, since results show no significant variations throughout time. This is confirmed by other studies conducted where the mechanical properties of iron are stable until they reach a point where they start to decrease and become compromised [55].

As the immersion time increases, both samples experience a higher density of calcium (and/or Fe) phosphate formation along with the formation of oxides/hydroxides. This is accompanied by a change in the morphology of the surface products from elongated particles into isolated powdery particles.

Regarding the samples produced at higher temperature (400 °C), both phenomena also occur, but Ca (and Fe) phosphates formation occurs even for the short immersion period (7 days), revealing a more uniform overall mechanism of material degradation. The formation of precipitates is much more intense than in the previous samples, resulting in complete covering of the material's surface, which suggests a higher bioactivity of this sample.

The corrosion process of iron in the presence of chlorine-content environment, starts with reactions described in Chapter 3.1, but the ferritic hydroxide (*Eq. 5*) is very unstable, especially in the presence of chlorine, so the following reaction is most likely to occur [56]:



The FeO(OH) compound has several phases and, depending on the surrounding environment conditions, such as oxygen concentration, salinity, pH, etc, some phases will have more tendency to form [57]. In fact, the chlorine content can affect the characteristics of the corrosion products in terms of structure and composition [58].

As found in previous studies [59], the phase with higher tendency to precipitate on the surface of the samples in the present study is the gamma phase (γ -FeO(OH)). The precipitated structures observed by SEM in this work are very similar to those of by Smith et al. [59], that studied the phenomenon of the nucleation of such structures in the presence of salt containing environment.

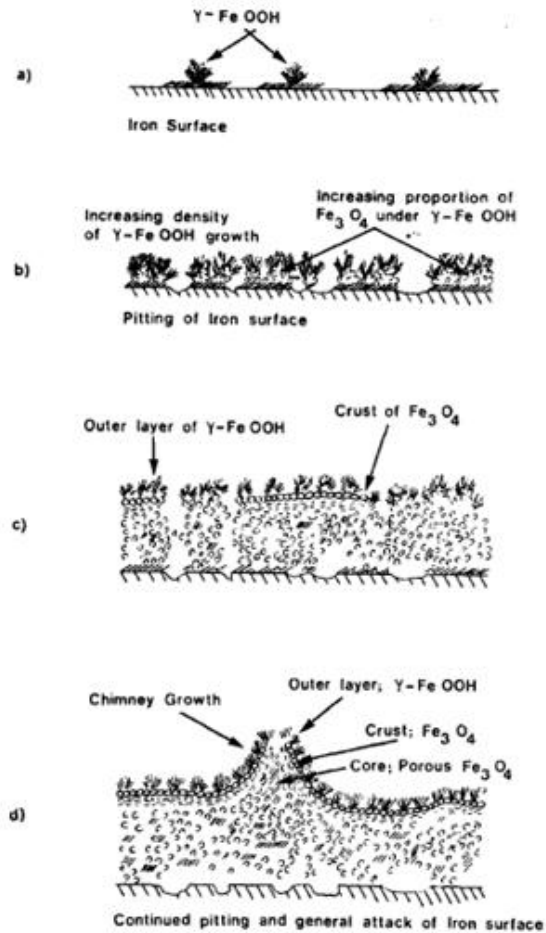


Figure 24: Schematic of corrosion mechanism of iron in salt water at 50 °C after: a) 10 minutes; b) 180 minutes; c) 360 minutes; d) 27 hours [59]

Figure 24 illustrates the mechanism of corrosion that was proposed to occur at the surface of iron samples in a chlorine containing environment. The nucleation of directional structures on the surface (as observed in the samples processed at 100 °C and 200 °C at short immersion periods) allied with the formation of columns (as observed in the samples processed at 400 °C immersed for longer periods) are in good agreement with the existence of such mechanism in the samples tested in the present study.

The conditions of the this study [59] were quite different from the ones presented in this thesis, however, a temperature and salinity dependence was noticed. The increased temperature and salinity seemed to accelerate the precipitation of the gamma phase on the surface. In the previous case, experiments were conducted in salt water at 50 °C. The structures started nucleating after 180 minutes and the columnar growth was present after 27 hours. Whereas, in this study, the temperature used for the immersion tests was 37 °C, and the concentration of salt in Hank's solution was lower than in salt water.

Nevertheless, it is clear a slower nucleation rate for the precipitate structures was found in the present study, taking 15 days for such precipitates to be observed and, 30 days for the columns to be developed was observed.

In another study on iron corrosion [58], performed at room temperature, the authors reported a period of 3 months for such structure to nucleate on the surface, which confirms the strong dependence of the precipitate formation on the solution temperature.

A deeper understanding of the mechanisms of degradation during immersion of the materials developed in the present study would require a more detailed analysis of the precipitates formed at the surface and of the immersion solution. This could be accomplished by x-ray diffraction and Raman spectroscopy analysis on the surface of the corroded samples, so as to find out, what species were released to the surrounding environment and what species are present on the surface of the samples. However, these analyses were out of the scope of the present thesis.

In conclusion, the corrosion rate of iron was improved by means of the incorporation of porosity in the samples, however, the compromise in mechanical properties was too extensive, making this material unsuitable to be used in orthopaedic applications.

7. Conclusions and future work

Samples of pure iron were prepared using hot pressing technique in order to find the suitability of this material as a biodegradable material for orthopaedic applications.

Hot pressing was proven to be a suitable technique for porous iron-based materials. This process allowed the control of porosity by means of adjusting the operating temperature of the process, producing materials with levels of porosity that decrease from 56% to 39% with increasing temperature from 100 °C to 400 °C.

The degradation of these materials in Hank's balanced salt solution was evaluated and its mechanisms assessed.

The results show that porosity improved the corrosion rate - the problem encountered in previous studies regarding iron as a biodegradable material. However, the high levels of porosity and low temperature sintering resulted in materials with low strength that compromised their mechanical properties, making them unsuitable to be used as implant materials for orthopaedic devices.

A need remains to further investigate these materials. Future studies should focus on increasing mechanical properties of iron, while maintaining the corrosion rate achieved in this work. This could be accomplished by reducing the amount of porosity and by sintering at higher temperatures to improve the strength.

Longer-term degradation tests should be carried out, also, in order to assess the material evolution during over the duration that it has to stay in the human body (about 1 year).

Finally, cell compatibility tests should be performed, as well, so as to assess cell reactions to the corrosion products of the implant.

8. References

1. Ratner, B. D., Hoffman, A. S., Schoen, F. J., and Lemons, J. E., *Biomaterials Science: An Introduction to Materials in Medicine*. 2012: Academic Press.
2. Hermawan, H., *Biodegradable Metals: From Concept to Applications*. 2012: Springer.
3. Peuster, M., Beerbaum, P., Bach, F. W., and Hauser, H., *Are resorbable implants about to become a reality?* *Cardiol Young*, 2006. **16**(2): p. 107-16.
4. Yeung, K. W. and Wong, K. H., *Biodegradable metallic materials for orthopaedic implantations: A review*. *Technology and Health Care*, 2012. **0**: p. 1-18.
5. Zheng, Y. F., Gu, X. N., and Witte, F., *Biodegradable metals*. *Materials Science and Engineering: R*, 2014. **77**: p. 1-34.
6. Yusop, A. H., Bakir, A. A., Shaharom, N. A., Abdul Kadir, M. R., and Hermawan, H., *Porous biodegradable metals for hard tissue scaffolds: a review*. *Int J Biomater*, 2012. **2012**: p. 641430.
7. Moravej, M. and Mantovani, D., *Biodegradable metals for cardiovascular stent application: interests and new opportunities*. *Int J Mol Sci*, 2011. **12**(7): p. 4250-70.
8. Bauer, S., Schmuki, P., von der Mark, K., and Park, J., *Engineering biocompatible implant surfaces*. *Progress in Materials Science*, 2013. **58**(3): p. 261-326.
9. Schomig, A., Kastrati, A., Mudra, H., Blasini, R., Schühlen, H., Klauss, V., Richardt, G., and Neumann, F. J., *Four-year experience with Palmaz-Schatz stenting in coronary angioplasty complicated by dissection with threatened or present vessel closure*. *Circulation*, 1994. **90**(6): p. 2716-2724.
10. Hermawan, H., Dube, D., and Mantovani, D., *Developments in metallic biodegradable stents*. *Acta Biomater*, 2010. **6**(5): p. 1693-7.
11. Wegener, B., Sievers, B., Utschneider, S., Müller, P., Jansson, V., Rößler, S., Nies, B., Stephani, G., Kieback, B., and Quadbeck, P., *Microstructure, cytotoxicity and corrosion of powder-metallurgical iron alloys for biodegradable bone replacement materials*. *Materials Science and Engineering: B*, 2011. **176**(20): p. 1789-1796.
12. Ramsden, J. J., Allen, D. M., Stephenson, D. J., Alcock, J. R., Peggs, G. N., Fuller, G., and Goch, G., *The Design and Manufacture of Biomedical Surfaces*. *Annals of the CIRP*, 2007. **56**(2): p. 687-711.
13. Mani, G., Feldman, M. D., Patel, D., and Agrawal, C. M., *Coronary stents: a materials perspective*. *Biomaterials*, 2007. **28**(9): p. 1689-710.
14. Lieu, P. T., M., H., Peterson, P. A., and Yang, Y., *The roles of iron in health and disease*. *Molecular Aspects of Medicine*, 2001(22): p. 1-87.
15. Colombo, A. and Karvouni, E., *Biodegradable Stents : "Fulfilling the Mission and Stepping Away"*. *Circulation*, 2000. **102**(4): p. 371-373.
16. Erne, P., Schier, M., and Resink, T. J., *The road to bioabsorbable stents: reaching clinical reality?* *Cardiovasc Intervent Radiol*, 2006. **29**(1): p. 11-6.
17. O'Brien, B. and Carroll, W., *The evolution of cardiovascular stent materials and surfaces in response to clinical drivers: a review*. *Acta Biomater*, 2009. **5**(4): p. 945-58.
18. Sammel, A. M., Chen, D., and Jepson, N., *New generation coronary stent technology--is the future biodegradable?* *Heart, Lung and Circulation*, 2013. **22**(7): p. 495-506.
19. Peuster, M., Hesse, C., Schloo, T., Fink, C., Beerbaum, P., and von Schnakenburg, C., *Long-term biocompatibility of a corrodible peripheral iron stent in the porcine descending aorta*. *Biomaterials*, 2006. **27**(28): p. 4955-62.
20. Waksman, R., Pakala, R., Baffour, R., Seabron, R., Hellinga, D., and Tio, F. O., *Short-term effects of biocorrosible iron stents in porcine coronary arteries*. *J Interv Cardiol*, 2008. **21**(1): p. 15-20.
21. Zhang, E., Chen, H., and Shen, F., *Biocorrosion properties and blood and cell compatibility of pure iron as a biodegradable biomaterial*. *J Mater Sci: Mater Med*, 2010. **21**(7): p. 2151-63.

22. Moravej, M., Purnama, A., Fiset, M., Couet, J., and Mantovani, D., *Electroformed pure iron as a new biomaterial for degradable stents: in vitro degradation and preliminary cell viability studies*. *Acta Biomater*, 2010. **6**(5): p. 1843-51.
23. Zhu, S., Huang, N., Xu, L., Zhang, Y., Liu, H., Sun, H., and Leng, Y., *Biocompatibility of pure iron: In vitro assessment of degradation kinetics and cytotoxicity on endothelial cells*. *Materials Science and Engineering: C*, 2009. **29**(5): p. 1589-1592.
24. Chao, W., Hong, Q., Xiao-ying, H., Ying-mao, R., Yi, T., Yan, C., Xin-lin, X., Liang, X., Yue, T., and Run-lin, G., *Short-term safety and efficacy of the biodegradable iron stent in mini-swine coronary arteries*. *Chinese Medical Journal*, 2013. **126**(24): p. 4752-4757.
25. Nie, F. L., Zheng, Y. F., Wei, S. C., Hu, C., and Yang, G., *In vitro corrosion, cytotoxicity and hemocompatibility of bulk nanocrystalline pure iron*. *Biomed Mater*, 2010. **5**(6): p. 1-10.
26. Oriňáková, R., Oriňák, A., Bučková, L. M., Giretová, M., Medvecký, L., Labbanczová, E., Kupková, M., Hrubovčáková, M., and Koval, K., *Iron Based Degradable Foam Structures for Potential Orthopedic Applications*. *International Journal of Electrochemical Science*, 2013. **8**: p. 12451 - 12465.
27. Papanikolaou, G. and Pantopoulos, K., *Iron metabolism and toxicity*. *Toxicol Appl Pharmacol*, 2005. **202**(2): p. 199-211.
28. Halliwell, B. and Gutteridge, J. M. C., *Biological relevant metal ion-dependent hydroxyl radical generation: An update*. *Federation of European Biochemical Societies*, 1992. **307**(1): p. 108-112.
29. Lobo, V., Patil, A., Phatak, A., and Chandra, N., *Free radicals, antioxidants and functional foods: Impact on human health*. *Pharmacognosy Review*, 2010. **4**(8): p. 118-26.
30. Jomova, K. and Valko, M., *Advances in metal-induced oxidative stress and human disease*. *Toxicology*, 2011. **283**(2-3): p. 65-87.
31. Mueller, P. P., May, T., Perz, A., Hauser, H., and Peuster, M., *Control of smooth muscle cell proliferation by ferrous iron*. *Biomaterials*, 2006. **27**(10): p. 2193-200.
32. Peuster, M., Wohlsein, P., Brüggmann, M., Ehlerding, M., Seidler, K., Fink, C., Brauer, H., Fischer, A., and Hausdorf, G., *A novel approach to temporary stenting: degradable cardiovascular stents produced from corrodible metal—results 6–18 months after implantation into New Zealand white rabbits*. *Heart*, 2001. **86**: p. 563-569.
33. Mueller, P. P., Arnold, S., Badar, M., Bormann, D., Bach, F. W., Drynda, A., Meyer-Lindenberg, A., Hauser, H., and Peuster, M., *Histological and molecular evaluation of iron as degradable medical implant material in a murine animal model*. *Journal of Biomedical Materials Research A*, 2012. **100**(11): p. 2881-9.
34. Moravej, M., Prima, F., Fiset, M., and Mantovani, D., *Electroformed iron as new biomaterial for degradable stents: development process and structure-properties relationship*. *Acta Biomater*, 2010. **6**(5): p. 1726-35.
35. Choi, J.-P., Lyu, H.-G., Lee, W.-S., and Lee, J.-S., *Densification and microstructural development during sintering of powder injection molded Fe micro-nanopowder*. *Powder Technology*, 2014. **253**: p. 596-601.
36. Kupková, M., Hrubovčáková, M., Oriňáková, R., Turoňová, A. M., and Zeleňák, A., *Corrosion Properties of Iron and Iron-Manganese Sintered Materials*. *Powder Metallurgy Progress*, 2013. **13**(1): p. 22-28.
37. Hermawan, H., Alamdari, H., Mantovani, D., and Dubé, D., *Iron–manganese: new class of metallic degradable biomaterials prepared by powder metallurgy*. *Powder Metallurgy*, 2008. **51**(1): p. 38-45.
38. Hermawan, H., Dube, D., and Mantovani, D., *Degradable metallic biomaterials: design and development of Fe-Mn alloys for stents*. *Journal of Biomedical Materials Research*, 2010. **93**(1): p. 1-11.
39. Hermawan, H., Dubé, D., and Mantovani, D., *Development of Degradable Fe-35Mn Alloy for Biomedical Application*. *Advanced Materials Research*, 2007. **15-17**: p. 107-112.
40. Hermawan, H. and Mantovani, D., *Process of prototyping coronary stents from biodegradable Fe-Mn alloys*. *Acta Biomater*, 2013. **9**(10): p. 8585-92.

41. Miura, H. and Matsuda, M., *Superhigh Strength Metal Injection Molded Low Alloy Steels by In-Process Microstructural Control*. Materials Transactions, 2002. **43**(3): p. 343-347.
42. Chou, D. T., Wells, D., Hong, D., Lee, B., Kuhn, H., and Kumta, P. N., *Novel processing of iron-manganese alloy-based biomaterials by inkjet 3-D printing*. Acta Biomater, 2013. **9**(10): p. 8593-603.
43. Lee, P. W., Trudel, Y., Iacocca, R., German, R. M., Ferguson, B. L., Eisen, W. B., Moyer, K., Madan, D., and Sanderow, H., *ASM Handbook Volume 7: Powder Metal Technologies and Applications*. 1998: ASM International.
44. Hu, C., Li, F., Qu, D., Wang, Q., Xie, R., Zhang, H., Peng, S., Bao, Y., and Zhou, Y., *Developments in hot pressing (HP) and hot isostatic pressing (HIP) of ceramic matrix composites*. 2014.
45. Jones, W. D., *Fundamental principles of powder metallurgy*. 1960: Edward Arnold Publishers LTD.
46. Tullborg, E.-L. and Larson, S. Å., *Porosity in crystalline rocks – A matter of scale*. Engineering Geology, 2006. **84**(1-2): p. 75-83.
47. *ASTM Standard B963-13 - Oil Content, Oil-Impregnation Efficiency, and Interconnected Porosity of Sintered Powder Metallurgy (PM) Products Using Archimedes' Principle*. 2013.
48. Degnan, C. C., Kennedy, A. R., and Shipway, P. H., *Fracture toughness measurements of powder metallurgical (P/M) green compacts: A novel method of sample preparation*. Materials Science, 2004. **39**: p. 2605– 2607.
49. Degnan, C. C., Shipway, P. H., and Kennedy, A. R., *Comparison of the green strength of warm compacted Astaloy CrM and Distaloy AE Densmix* powder compacts*. Materials Science and Technology, 2004. **20**(6): p. 731-738.
50. Jonsén, P., Häggblad, H. Å., and Sommer, K., *Tensile strength and fracture energy of pressed metal powder by diametral compression test*. Powder Technology, 2007. **176**(2-3): p. 148-155.
51. *ASTM Standard D3967-08 - Splitting Tensile Strength of Intact Rock Core Specimens*. 2008.
52. Fan, X., Chen, J., Zou, J.-p., Wan, Q., Zhou, Z.-c., and Ruan, J.-m., *Bone-like apatite formation on HA/316L stainless steel composite surface in simulated body fluid*. Transactions of Nonferrous Metals Society of China, 2009. **19**(2): p. 347-352.
53. Kokubo, T., *Apatite formation on surfaces of ceramics, metals and polymers in body environment*. Acta Metallurgica, 1998. **46**(7): p. 2519-2527.
54. Pisarek, M., Roguska, A., Andrzejczuk, M., Marcon, L., Szunerits, S., Lewandowska, M., and Janik-Czachor, M., *Effect of two-step functionalization of Ti by chemical processes on protein adsorption*. Applied Surface Science, 2011. **257**(19): p. 8196-8204.
55. Garbatov, Y., Guedes Soares, C., Parunov, J., and Kodvanj, J., *Tensile strength assessment of corroded small scale specimens*. Corrosion Science, 2014. **85**: p. 296-303.
56. Singh, D. D. N., Yadav, S., and Saha, J. K., *Role of climatic conditions on corrosion characteristics of structural steels*. Corrosion Science, 2008. **50**(1): p. 93-110.
57. Pérez, F. R., Barrero, C. A., and García, K. E., *Factors affecting the amount of corroded iron converted into adherent rust in steels submitted to immersion tests*. Corrosion Science, 2010. **52**(8): p. 2582-2591.
58. Ma, Y., Li, Y., and Wang, F., *Corrosion of low carbon steel in atmospheric environments of different chloride content*. Corrosion Science, 2009. **51**(5): p. 997-1006.
59. Smith, D. C. and McEnaney, B., *The Influence of dissolved oxygen concentration on the corrosion of grey cast iron in water at 50 °C*. Corrosion Science, 1979. **19**: p. 379-394.